AN INVESTIGATION INTO THE TOTAL DISSOLVED GAS DYNAMICS OF THE WELLS PROJECT
(Total Dissolved Gas Investigation)

WELLS HYDROELECTRIC PROJECT

FERC NO. 2149

INTERIM REPORT
REQUIRED BY FERC

September 2008

Prepared by:
M. Politano, A. Arenas Amado and L. Weber
IIHR-Hydroscience & Engineering
The University of Iowa
300 South Riverside Drive
Iowa City, Iowa 52242-1585

Prepared for:
Public Utility District No. 1 of Douglas County
East Wenatchee, Washington

For copies of this Study Report, contact:

Public Utility District No. 1 of Douglas County
Attention: Relicensing
1151 Valley Mall Parkway
East Wenatchee, WA 98802-4497
Phone: (509) 884-7191
E-Mail: relicensing@dcpud.org

Table of Contents

List of Tables

List of Figures

List of Appendices

ABSTRACT

The current Wells Hydroelectric Project (Wells Project) license will expire on May 31, 2012. As part of the Wells Project relicensing process, the Public Utility District No. 1 of Douglas County (Douglas PUD) is required to obtain a water quality certificate pursuant to Section 401 of the Clean Water Act. As part of the 401 certification process, the Washington State Department of Ecology (Ecology) must determine whether the Wells Project is in compliance with state water quality standards, including the numeric standards, for total dissolved gas (TDG).

Douglas PUD examined TDG production dynamics at the Wells Project to comply with State water quality standards (WQS). As part of the relicensing of the Wells Project, Douglas PUD has initiated a series of assessments aimed at gaining a better understanding of the effect of spill operations on the production, transport and mixing of TDG in the Wells Dam tailrace.

The primary goal of this study was to develop an unsteady three-dimensional (3D) two-phase flow computational fluid dynamics (CFD) tool to predict the hydrodynamics and TDG distribution within the Wells tailrace. Two models were used in the study; a volume of fluid (VOF) model and a rigid-lid two-phase flow model.

The VOF model predicts the flow regime and the free-surface characteristics, recognizing that a spillway jet may plunge to depth in the tailrace or remain closer to the surface depending upon the geometry of the outlet and the tailwater elevation. The VOF model boundary extended approximately 1,700 ft downstream of the dam.

The rigid-lid model included 16,500 ft of the Wells tailrace, from Wells Dam downstream to the TDG compliance monitoring station. This two-phase flow model characterizes the hydrodynamics and three-dimensional distribution of gas volume fraction, bubble size and TDG in the Wells tailrace. This model assumes that the free surface can be modeled using a rigid-lid non-flat boundary condition. The free-surface shape for the first 1,000 feet downstream of the dam was extracted from VOF computations and slopes derived from HEC-RAS simulations were used for the downstream region. The upstream velocity profiles derived from the VOF model were input to the rigid-lid model. The gas volume fraction and bubble diameter at the spillbays are the external parameters of the model.

The model was calibrated and validated using field data collected in 2006 during a TDG production dynamics study (EES et al. 2007). The model was then calibrated using data collected during spill tests conducted on June 4 and June 5, 2006. The spillway flow was spread across spillbays on June 4 and concentrated through a single spillbay on June 5. Agreement was attained between the depth-averaged velocity data collected in the field and those generated by the model. A gas volume fraction of 3% and bubble diameter of 0.5 mm in the spillbays produced TDG values that bracketed the 2006 field observations.

Once calibrated, the predictive ability of the model was validated by running the model for three different operational conditions tested in 2006. The model captured the lateral TDG distribution and the reduction of TDG longitudinally as observed in the field. The numerical results demonstrate that the model provides a reliable predictor of tailrace TDG and therefore can be

used as a tool to identify Project operations that can minimize TDG concentrations downstream of Wells Dam.

1.0 INTRODUCTION

1.1 General Description of the Wells Hydroelectric Project

The Wells Hydroelectric Project (Wells Project) is located at river mile (RM) 515.6 on the Columbia River in the State of Washington (Figure 1.1-1). Wells Dam is located approximately 30 river miles downstream from the Chief Joseph Hydroelectric Project, owned and operated by the United States Army Corps of Engineers (COE), and 42 miles upstream from the Rocky Reach Hydroelectric Project, owned and operated by Public Utility District No. 1 of Chelan County (Chelan PUD). The nearest town is Pateros, Washington, which is located approximately 8 miles upstream from the Wells Dam.

The Wells Project is the chief generating resource for the Public Utility District No. 1 of Douglas County (Douglas PUD). It includes ten generating units with a nameplate rating of 774,300 kW and a peaking capacity of approximately 840,000 kW. The design of the Wells Project is unique in that the generating units, spillways, switchyard, and fish passage facilities were combined into a single structure referred to as the hydrocombine. Fish passage facilities reside on both sides of the hydrocombine, which is 1,130 feet long, 168 feet wide, with a crest elevation of 795 feet msl.

The Wells Reservoir is approximately 30 miles long. The Methow and Okanogan rivers are tributaries of the Columbia River within the Wells Reservoir. The Wells Project boundary extends approximately 1.5 miles up the Methow River and approximately 15.5 miles up the Okanogan River. The surface area of the reservoir is 9,740 acres with a gross storage capacity of 331,200 acre-feet and usable storage of 97,985 acre feet at the normal maximum water surface elevation of 781 above mean sea level (msl) (Figure 1.1-1).

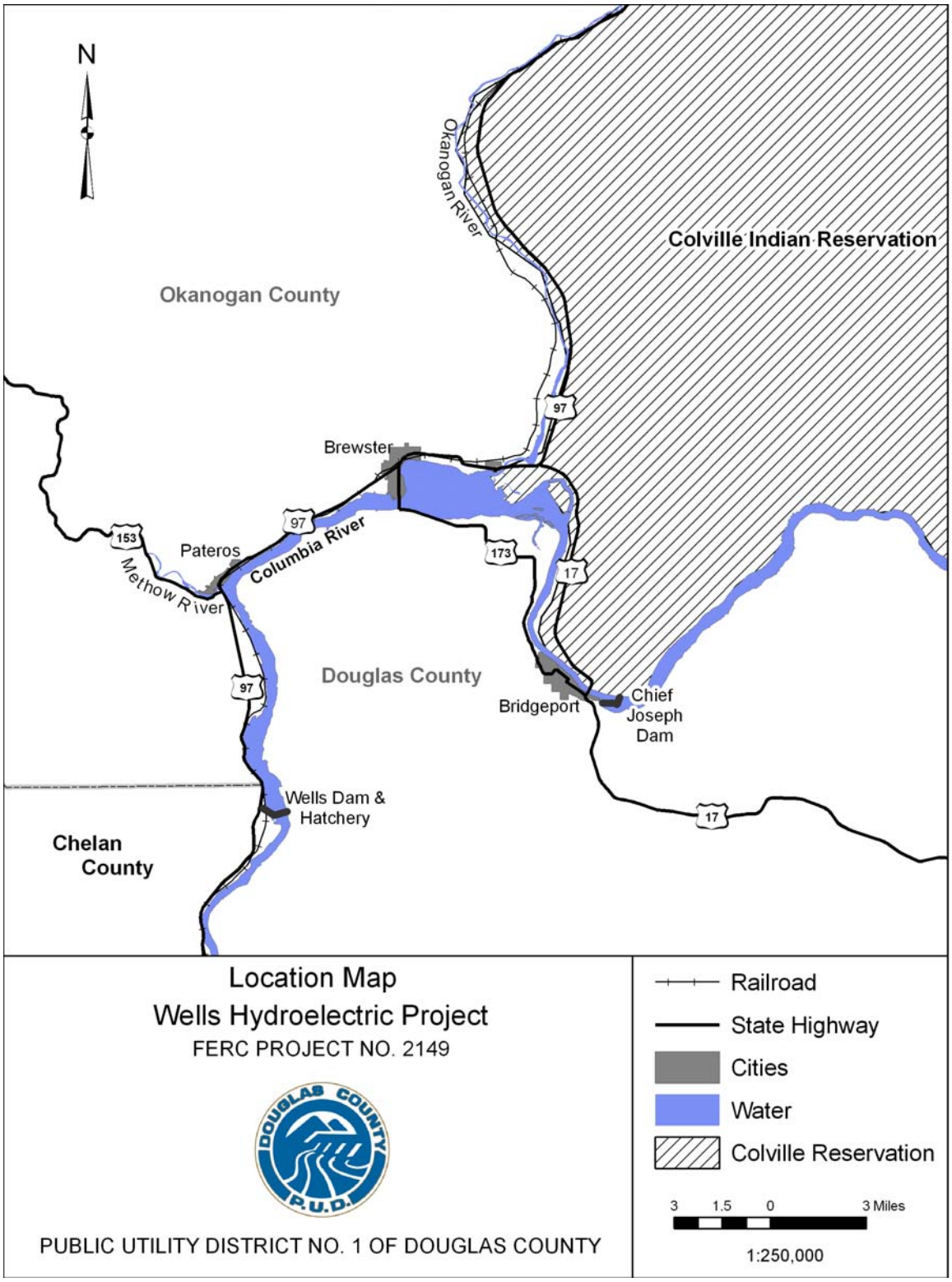

Figure 1.1-1 Location Map of the Wells Hydroelectric Project.

1.2 Relicensing Process

The current Wells Project license will expire on May 31, 2012. Douglas PUD is using the Integrated Licensing Process (ILP) promulgated by Federal Energy Regulatory Commission (FERC) Order 2002 (18 CFR Part 5). Stakeholders consisting of representatives from state and federal agencies, tribes, local governments, non-governmental organizations and the general public have participated in the Wells Project ILP, from a very early stage, to identify information needs related to the relicensing of the Wells Project.

In August 2005, Douglas PUD initiated a series of Resource Work Group (RWG) meetings with stakeholders regarding the upcoming relicensing of the Wells Project. This voluntary effort was initiated to provide stakeholders with information about the Wells Project, to identify resource issues and to develop preliminary study plans prior to filing the Notice of Intent (NOI) and Pre-Application Document (PAD). The RWGs were formed to discuss issues related to the Wells Project and its operations.

The primary goals of the RWGs were to identify resource issues and potential study needs in advance of Douglas PUD filing the NOI and PAD. Through 35 meetings, each RWG cooperatively developed a list of Issue Statements, Issue Determination Statements and Agreed-Upon Study Plans. An Issue Statement is an agreed-upon definition of a resource issue raised by a stakeholder. An Issue Determination Statement reflects the RWG's efforts to apply FERC's seven study criteria to mutually determine the applicability of each individual Issue Statement. Agreed-Upon Study Plans are the finished products of the informal RWG process.

Douglas PUD submitted the NOI and PAD to FERC on December 1, 2006. The PAD included the RWGs' 12 Agreed-Upon Study Plans. The filing of these documents initiated the relicensing process for the Wells Project under FERC's regulations governing the ILP.

On May 16, 2007, Douglas PUD submitted a Proposed Study Plan (PSP) Document. The PSP Document consisted of the Applicant's Proposed Study Plans, Responses to Stakeholder Study Requests and a schedule for conducting the Study Plan Meeting. The ILP required Study Plan Meeting was conducted on June 14, 2007. The purpose of the Study Plan Meeting was to provide stakeholders with an opportunity to review and comment on Douglas PUD's PSP Document, to review and answer questions related to stakeholder study requests and to attempt to resolve any outstanding issues with respect to the PSP Document.

On September 14, 2007, Douglas PUD submitted a Revised Study Plan (RSP) Document. The RSP Document consisted of a summary of each of Douglas PUD's revised study plans and a response to stakeholder PSP Document comments.

On October 11, 2007, FERC issued its Study Plan Determination based on its review of the RSP Document and comments from stakeholders. FERC's Study Plan Determination required Douglas PUD to complete 10 of the 12 studies included in its RSP Document. Douglas PUD has opted to complete all 12 studies to better prepare for the 401 Water Quality Certification process conducted by the Washington State Department of Ecology and to fulfill its commitment to the RWGs who collaboratively developed the 12 Agreed-Upon Study Plans with Douglas PUD.

These study plans have been implemented during the designated ILP study period. The results from the study plans have been developed into 12 Study Reports. Each report is included in Douglas PUD's Initial Study Report (ISR) Document, which is scheduled for filing with FERC on October 15, 2008.

This interim report provides initial results from the Total Dissolved Gas Investigation. Additional modeling efforts are still underway. The final report will be completed and available to the public in early 2009.

There were no variances from the FERC approved study plan for the Total Dissolved Gas Investigation.

1.3 Overview of Total Dissolved Gas at Wells Dam

The Columbia and Snake river basins are the most productive sources of hydropower in the United States. The Wells Dam, which is owned and operated by Douglas PUD, is located at RM 515.6 on the Columbia River, Washington (Figure 1.3-1). The spillway gates at Wells Dam are used to pass water when river flows exceed the maximum powerhouse capacity (forced spill), to assist outmigration of juvenile salmonids (fish bypass spill), and to prevent flooding along the mainstem Columbia River (flood control spill). Forced spill occurs when the total flow is in excess of the powerhouse hydraulic capacity. The Wells Project can pass 19.5 kcfs through each operating turbine (195 kcfs in 10 turbines) with an additional 10 kcfs used to operate the juvenile fish bypass system (ASL 2007). Therefore, spill is forced when the inflows are higher than 205 kcfs. Spill may occur at flows less than the hydraulic capacity when the volume of water is greater than the amount required to meet electric power system loads. Hourly coordination among hydroelectric projects on the mid-Columbia River was established to minimize the latter situation for spill.

Wells Dam is a hydrocombine-designed dam with the spillway situated directly above the powerhouse. Research at Wells Dam in the mid-1980s showed that a modest amount of spill would effectively guide between 92 percent and 96 percent of the downstream migrating juvenile salmonids through the Juvenile Bypass System (JBS) and away from the turbines. The operation of the Wells JBS utilizes five spillways that have been modified with constricting barriers to improve the attraction flow while using modest levels of water (Klinge 2005). The JBS will typically use approximately 6-8 percent of the total river flow for fish guidance. The high level of fish protection at Wells Dam has won the approval of the fisheries agencies and tribes and was vital to the recently approved Anadromous Fish Agreement and Habitat Conservation Plan (HCP).

State of Washington water quality standards require TDG levels to not exceed 110% at any point of measurement. Due to air entrainment in the plunge pools below spillways, TDG levels can sometimes exceed the State's standard during spill events at dams. The exceptions to the State's standard when levels are allowed to be exceeded are (1) to pass flood flows at the Project and (2) to pass voluntary spill to assist out migrating juvenile salmonids. The 7Q10 flood flow, which is defined as the highest average flow that occurs for seven consecutive days in a once-in-ten-year period, is 246 kcfs at the Wells Project. Considering that 175.5 kcfs can be passed through nine

of the ten turbines at Wells, 10 kcfs through the juvenile fish bypass system and 1 kcfs in the fishway, spillway bays must pass 59.5 kcfs in the 7Q10 flood flow.

Figure 1.3-1 Map of Washington showing the location of the Wells Dam

2.0 GOALS AND OBJECTIVES

The goal of this study is to develop a numerical model capable of predicting the hydrodynamics and TDG concentrations in the tailrace of the Wells Project. The purpose of the model is to assist in the understanding of the underlying phenomena leading to TDG supersaturation allowing the evaluation of the effectiveness of spill type and plant operations in reducing TDG production at Wells Dam.

3.0 STUDY AREA

The study area includes approximately 16,500 ft of the Wells tailrace, extending from Wells Dam downstream to transect TW3 (Transect T3) (Figure 3.0-1). Transect TW3 coincides with the TDG compliance monitoring station.

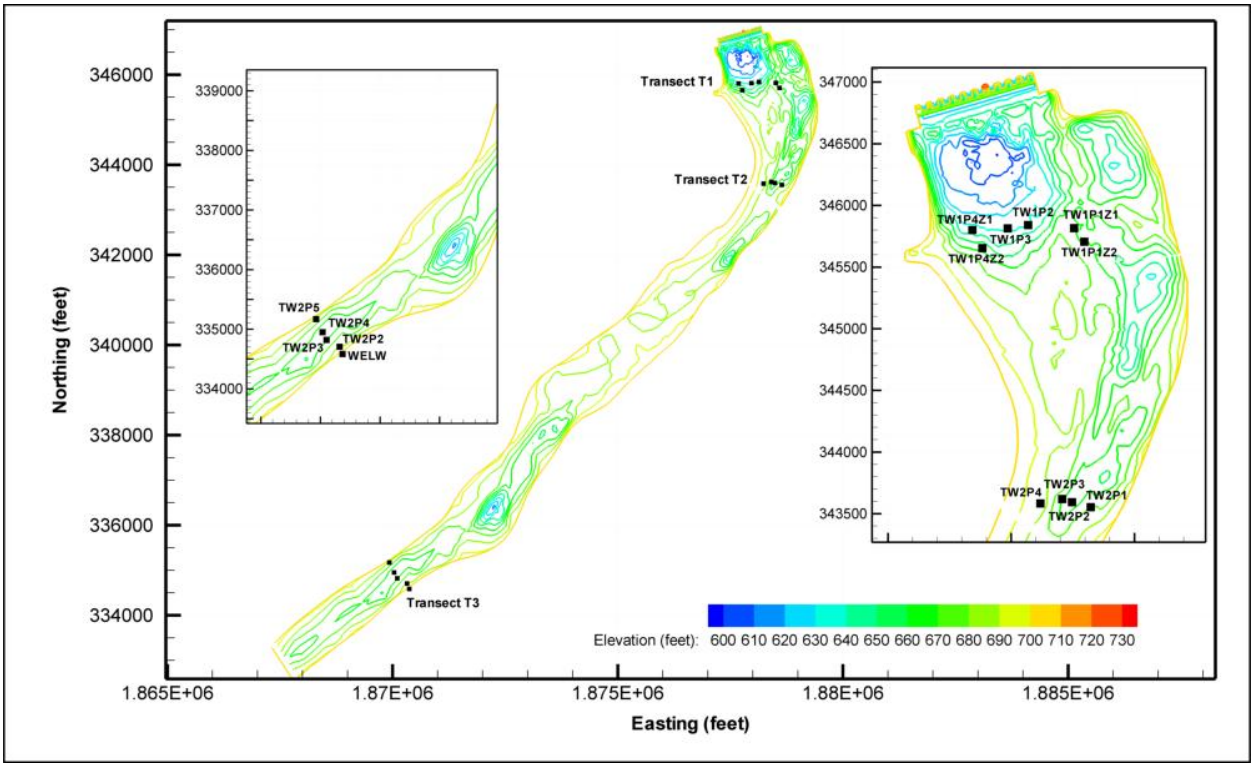

Figure 3.0-1 Study Area for the TDG model

4.0 BACKGROUND AND EXISTING INFORMATION

4.1 Summary of TDG studies in the Wells Tailrace

Douglas PUD conducted a series of assessments aimed at gaining a better understanding of TDG production dynamics resulting from spill operations at Wells Dam. Each year from 2003 to 2008, Douglas PUD has performed experimental spill operations to understand the relationship between water spilled over the dam and the production of TDG.

In 2003 and 2004, Columbia Basin Environmental (CBE) deployed TDG sensors along two transects downstream of Wells Dam. The objectives of this study were to determine the effectiveness of the tailwater sensor and better understand the relationship between spillway releases and TDG production (CBE 2003, 2004). In a two-week period, the studies showed that the tailwater station provided a reliable record of daily average TDG values in the Wells Dam tailrace.

In spring 2005, Douglas PUD conducted a study to measure TDG pressures resulting from various spill patterns at Wells Dam (CBE, 2006). An array of water quality data loggers was installed in the Well tailrace for a period of two weeks between May 23, 2005 and June 6, 2005. The Wells powerhouse and spillway were operated through a controlled range of operational scenarios that varied both total flow and allocation of the spillway discharge. A total of eight configurations were tested including flat spill patterns (near equal distribution of spill across the

entire spillway), crowned spill patterns (spill is concentrated towards the center of the spillway), and spill over loaded and unloaded generating units. Results from the study indicated that spill from the west side of the spillway resulted in consistently higher TDG saturations than similar spill from the east side. Flat spill patterns yielded higher TDG saturations than crowned spill for similar total discharges. The results of this study also indicated that TDG levels of powerhouse flows may be influenced by spill.

In 2006, Douglas PUD continued TDG assessments at the Wells Project by examining alternative spill configurations and project operations to minimize the production of TDG. The purpose of the 2006 study was to evaluate how the Project could be operated to successfully pass the 7Q10 river flow while remaining in compliance with Washington State TDG standards. Thirteen sensors were placed along transects in the tailrace located at 1,000, 2,500 and 15,000 feet below Wells Dam. There were also three sensors placed across the forebay. The sensors were programmed to collect data in 15 minute intervals for both TDG and water temperature. Each test required the operations of the dam to maintain stable flows through the powerhouse and spillway for at least a three hour period. While there were 30 scheduled spill events, there were an additional 50 events where the powerhouse and spillway conditions were held constant for a minimum three hour period. These additional events provided an opportunity to collect TDG data on a variety of Project operations that met study criteria. These are included in the results of the 2006 TDG Abatement Study (EES et al., 2007). Spill amounts ranged from 5.2 to 52.0% of project flow and flows ranged from 2.2 to 124.7 kcfs for spill and 16.4 to 254.0 kcfs for total discharge. There were six tests that were performed at flows that exceeded the Wells Dam 7Q10 flows of 246 kcfs. Results of the study indicated that two operational scenarios, spread spill and concentrated spill (spill from 1 or 2 gates), produced the lowest levels of TDG. The 2006 study also indicated that the current location of the tailwater TDG compliance monitoring station is appropriate in providing representative TDG production information both longitudinally and laterally downstream of Wells Dam.

4.2 Numerical studies of TDG in Tailraces

Early studies to predict TDG below spillways were based on experimental programs and physical models (Hibbs and Gulliver 1997; Orlins and Gulliver 2000). The primary shortcoming of this approach is that the laboratory models cannot quantitatively predict the change in TDG due to model scaling issues. The approach relies on performance curves that relate flow conditions with past field experiences. This has led to inconsistent results at hydroelectric projects, some being quite successful while others less successful.

Computational fluid dynamics (CFD) modeling offers a powerful tool for TDG and hydrodynamics prediction. In the application to powerhouse/spillway flows, an understanding of the underlying physics and the capability to model three-dimensional physical phenomena is of paramount importance in performing reliable numerical studies. The most important source of TDG production is the gas transfer from the entrained bubbles, therefore a TDG predictive model must account for the two-phase flow in the stilling basin and the mass transfer between bubbles and water.

The TDG concentration depends on complex processes such as air entrainment in the spillway (pre-entrainment), entrainment when the jet impacts the tailwater pool, breakup and coalescence of entrained bubbles, mass transfer between bubbles and water, degasification at the free surface, and bubble and TDG transport. In addition, tailrace flows in the region near the spillway cannot be assumed to have a flat air/water interface which results in the required computation of the free surface shape. Moreover, it has been demonstrated that surface jets may cause a significant change in the flow pattern since they attract water toward the jet region, a phenomenon referred to as water entrainment (Liepmann 1990; Walker and Chen 1994; Walker 1997). Water entrainment leads to mixing and modification of the TDG field. As an additional complexity, the presence of bubbles has a strong effect on water entrainment. Bubbles reduce the density (and pressure) and effective viscosity in the spillway region and affect the liquid turbulence.

Free surface models can predict the shape and development of the free surface and, though costly, have feasible application to complex three dimensional (3D) flows. In the field of hydraulic engineering, free surface models are not yet widely applied but are steadily developing (Turan et al., 2008; Ferrari et. al., 2008). However, direct simulation of individual bubbles in a spillway/tailrace environment is well beyond current computer capabilities. Therefore, a two-fluid model with space-time averaged quantities that do not resolve the interface is needed to model the effect of the bubbles on the flow field and bubble dissolution. Numerical simulations of two phase flows using two-fluid models have been extensively used, mainly in the chemical and nuclear engineering community. Jakobsen et al. (2005) provided an extensive review of the state-of-the-art of two-phase flow modeling. Politano et al. (2007a) used a two-dimensional (2D) two-fluid model assuming isotropic turbulence to predict the gas distribution and TDG concentration in a cross-section passing through a spillway bay at Wanapum Dam. The model was compared against field data measured before deflector installation. The model allowed examination of the effect of the bubble size on TDG concentration. However, 2D simulations cannot capture the water entrainment caused by deflectors and therefore the TDG dilution due to powerhouse flows could not be predicted with the model. Turan et al. (2007) conducted the first numerical study to predict the hydrodynamics and water entrainment in a hydropower tailrace. The authors used an anisotropic mixture model that accounts for the gas volume fraction and attenuation of normal fluctuations at the free surface. Politano et al. (2007b) used an anisotropic mixture model for the 3D prediction of the two phase flow and TDG in the tailrace of Wanapum Dam. The simulations captured the measured water entrainment in the tailrace of Wanapum Dam. In this study, quantitative agreement between predicted and measured TDG was obtained for two different operational conditions.

4.3 Aquatic Resource Work Group

As part of the relicensing process for the Wells Project, Douglas PUD established an Aquatic Resource Work Group (Aquatic RWG) which began meeting informally in November, 2005. This voluntary effort was initiated to provide stakeholders with information about the Wells Project, to collaboratively identify potential resource issues related to Project operations and relevant to relicensing, and to develop preliminary study plans to be included in the Wells Pre-Application Document (PAD) (DCPUD, 2006).

Through a series of meetings, the Aquatic RWG cooperatively developed a list of Issue Statements, Issue Determination Statements and Agreed-Upon Study Plans. An Issue Statement is an agreed-upon definition of a resource issue raised by a stakeholder. An Issue Determination Statement reflects the RWGs' efforts to review the existing project information and to determine whether an issue matches with FERC's seven criteria and would be useful in making future relicensing decisions. Agreed-Upon Study Plans are the finished products of the informal RWG process.

Based upon these meetings and discussions, the Aquatic RWG proposed to conduct studies of the TDG dynamics of Wells Dam. The need for this study was agreed to by all members of the Aquatic RWG, including Douglas PUD. These studies are intended to inform future relicensing decisions, including the water quality certification process and will fill data gaps that have been identified by the Aquatic RWG.

The Issue Statement and Issue Determination Statement listed below were included in the PAD (section number included) filed with FERC on December 1, 2006:

4.3.1 Issue Statement (PAD Section 6.2.1.5)

Wells Dam may affect compliance with Total Dissolved Gas (TDG) standards in the Wells tailrace and Rocky Reach forebay.

4.3.2 Issue Determination Statement (PAD Section 6.2.1.5)

Wells Dam can have an effect on compliance with the TDG standard. The resource work group believes that additional information is necessary in the form of continued monitoring and that these data will be meaningful with respect to the State 401 Water Quality Certification process. Douglas PUD has been implementing studies at Wells Dam to address TDG production dynamics.

4.4 Project Nexus

TDG concentrations may become a water quality concern when gases supersaturate a river, lake or stream. The plunging water caused by spill at hydroelectric facilities may elevate TDG to levels that may result in impaired health or even death for aquatic life residing or migrating within the affected area.

The Washington State Department of Ecology (Ecology) is responsible for the protection and restoration of the state's waters. Ecology has adopted water quality standards that set limits on pollution in lakes, rivers, and marine waters in order to protect water quality. On July 1, 2003, Ecology completed the first major overhaul of the state's water quality standards in a decade. A significant revision presented in the 2003 water quality standards classifies fresh water by actual use, rather than by class as was done in the 1997 standards. These revisions were adopted in order to make the 2003 standards less complicated to interpret and provide future flexibility as the uses of a water body evolve.

The applicable water quality standard for TDG for the Columbia River at hydroelectric projects states:

- Total dissolved gas shall not exceed 110 percent of saturation at any point of sample collection.

However, as discussed in Section 4.0, an exception to the above standard is allowed to aid fish passage over hydroelectric dams when it is determined that this action is consistent with an Ecology-approved gas abatement plan. The information collected during this study will assist Douglas PUD in operating the Wells Project in a manner that minimizes TDG in the Wells tailrace and Rocky Reach forebay.

5.0 METHODOLOGY

5.1 Simulation Conditions

The performance of the model to predict the TDG distribution and hydrodynamics was evaluated using field data collected for a period of six weeks between May 14, 2006 and June 28, 2006, during the TDG production dynamics study (EES et al., 2007). Velocities were measured on three transects in the near field region of the Wells tailrace on June 4, 2006 and June 5, 2006. Figure 3.0-1 shows the 15 stations where TDG sensors were deployed during the field study.

5.1.1 Calibration

The model was calibrated against data collected on June 4 and June 5, 2006, referred to as treatments 46 and 47 in the report by EES et al. (2007). The spillway flow was spread across all spillbays on June 4 and concentrated in a single spillbay on June 5. Total river flows during these treatments were 172.4 kcfs and 222.3 kcfs, respectively. Tables 6.1-1 and 6.1-2 summarize plant operations, TDG saturation in the forebay, and tailwater elevation on these days. Powerhouse and spillway units are numbered from west to east.

Table 5.1-1 Conditions used for the numerical simulations of June 4, 2006

Treatment 46 S - June 4, 2006									
Tailwater Elevation: 717.3 ft									
Powerhouse Unit Discharge (kcfs)									
U1	U2	U3	U4	U5	U6	U7	U8	U9	U10
0.0	14.7	14.7	14.4	14.7	14.7	14.8	14.8	14.4	14.7
Powerhouse Total: 131.8 kcfs									
Spillway Unit Discharge (kcfs)									
S1	S2	S3	S4	S5	S6	S7	S8	S9	S10
0.0	1.6	5.4	5.2	5.4	5.2	5.4	5.2	5.4	1.6
Spillway Total: 40.6 kcfs									
Total River Flow: 172.4 kcfs									
Forebay TDG: 111.8%									

Table 5.1-2 Conditions used for the numerical simulations of June 5, 2006

Treatment 47 FG - June 5, 2006									
Tailwater Elevation: 720.2 ft									
Powerhouse Unit Discharge (kcfs)									
U1	U2	U3	U4	U5	U6	U7	U8	U9	U10
0.0	18.9	18.0	18.5	18.3	19.0	20.2	19.6	19.9	18.2
Powerhouse Total: 170.6 kcfs									
Spillway Unit Discharge (kcfs)									
S1	S2	S3	S4	S5	S6	S7	S8	S9	S10
0.0	1.3	0.0	2.2	0.0	2.2	42.5	2.2	0.0	1.3
Spillway Total: 51.7 kcfs									
Total River Flow: 222.3 kcfs									
Forebay TDG: 111.5%									

5.1.2 Numerical Model Validation

The predictive ability of the numerical model was validated using three different spillway conditions tested in 2006. The three spillway conditions are: treatment 1-Full Gate (FG); treatment 11-FG; and treatment 63-Concentrated (C). The FG designates the use of a single spill bay whereas C designates a crowned spill pattern. Plant operation and tailwater elevations associated with each of the treatments are tabulated on Tables 5.1-3 to 5.1-5.

Table 5.1-3 Conditions used for the numerical simulations of May 14, 2006

Treatment 1 FG - May 14, 2006									
Tailwater Elevation: 711.5 ft									
Powerhouse Unit Discharge (kcfs)									
U1	U2	U3	U4	U5	U6	U7	U8	U9	U10
0.0	15.0	15.0	14.8	0.0	0.0	0.0	0.0	14.8	15.2
Powerhouse Total: 74.8 kcfs									
Spillway Unit Discharge (kcfs)									
S1	S2	S3	S4	S5	S6	S7	S8	S9	S10
0.0	1.3	0.0	2.2	0.0	2.2	35.4	2.2	0.0	1.3
Spillway Total: 44.6 kcfs									
Total River Flow: 120.4 kcfs									
Forebay TDG: 109.1%									

Table 5.1-4 Conditions used for the numerical simulations of May 17, 2006

Treatment 11 FG - May 17, 2006									
Tailwater Elevation: 715.4 ft									
Powerhouse Unit Discharge (kcfs)									
U1	U2	U3	U4	U5	U6	U7	U8	U9	U10
0.0	18.9	19.1	18.7	19.2	0.0	0.0	0.0	18.7	19.2
Powerhouse Total: 113.7 kcfs									
Spillway Unit Discharge (kcfs)									
S1	S2	S3	S4	S5	S6	S7	S8	S9	S10
0.0	0.9	0.0	2.2	0.0	2.2	34.1	2.2	0.0	0.9
Spillway Total: 42.6 kcfs									
Total River Flow: 157.2 kcfs									
Forebay TDG: 110.4%									

Table 5.1-5 Conditions used for the numerical simulations of June 17, 2006

Treatment 63 C - June 17, 2006									
Tailwater Elevation: 718.6 ft									
Powerhouse Unit Discharge (kcfs)									
U1	U2	U3	U4	U5	U6	U7	U8	U9	U10
0.0	13.0	13.0	12.9	13.0	13.0	13.1	13.1	12.8	13.1
Powerhouse Total: 117.1 kcfs									
Spillway Unit Discharge (kcfs)									
S1	S2	S3	S4	S5	S6	S7	S8	S9	S10
0.0	1.7	0.0	2.2	0.0	2.2	29.8	19.9	29.8	1.7
Spillway Total: 87.4 kcfs									
Total River Flow: 205.5 kcfs									
Forebay TDG: 113.9%									

5.2 Model Overview

The models used in this study are based upon the general purpose CFD code FLUENT, which solves the discrete Reynolds Averaged Navier Stokes (RANS) equations using a cell centered finite volume scheme. Two models were used to predict the hydrodynamics and TDG distribution within the tailrace of the Wells Project: a volume of fluid (VOF) model and a rigid-lid non-flat lid model.

The VOF model predicted the flow regime and free-surface for the first 1,000 feet downstream of the dam. The free-surface shape was then used to generate a grid conformed to this geometry and fixed throughout the computation (rigid, non-flat lid approach). After the statistically-steady state was reached, the VOF solution that minimizes the difference between measured and predicted tailwater elevation was selected. Water surface elevations and local slopes derived from simulations using the Hydrologic Engineering Centers River Analysis System (HEC-RAS)

were used at the downstream region of the model. The HEC-RAS computations were performed using geometric input files provided by Douglas PUD with a roughness coefficient of 0.035.

The rigid-lid model allowed proper assessment of water entrainment and TDG concentration. The model assumed one variable bubble size, which could change due to local bubble/water mass transfer and pressure. The air entrainment (gas volume fraction and bubble size) was assumed to be a known inlet boundary condition. It must be noted that the choice of bubble size and volume fraction at the spillway bays has an important effect on the level of entrainment and TDG distribution. In this study a reasonable single-size bubble diameter and volume fraction were used at the spillway gates to bracket the experimental TDG data during the model calibration and the same values are used for all computations.

Specific two phase flow models and boundary conditions were implemented into FLUENT through User Defined Functions (UDFs). Two-phase User Defined Scalars (UDSs) transport equations were used to calculate the distribution of TDG and bubble number density.

The model included the main features of the Wells Dam, including the draft tube outlets of the generating units, spillway, top spill in bays 2 and 10 and fish passage facilities (Figure 5.2-1). Bathymetric data supplied by Douglas PUD were used to generate the river bed downstream of the dam. Detail of Figure 5.2-1 shows a cross section through a spillway unit illustrating the Wells Hydrocombine.

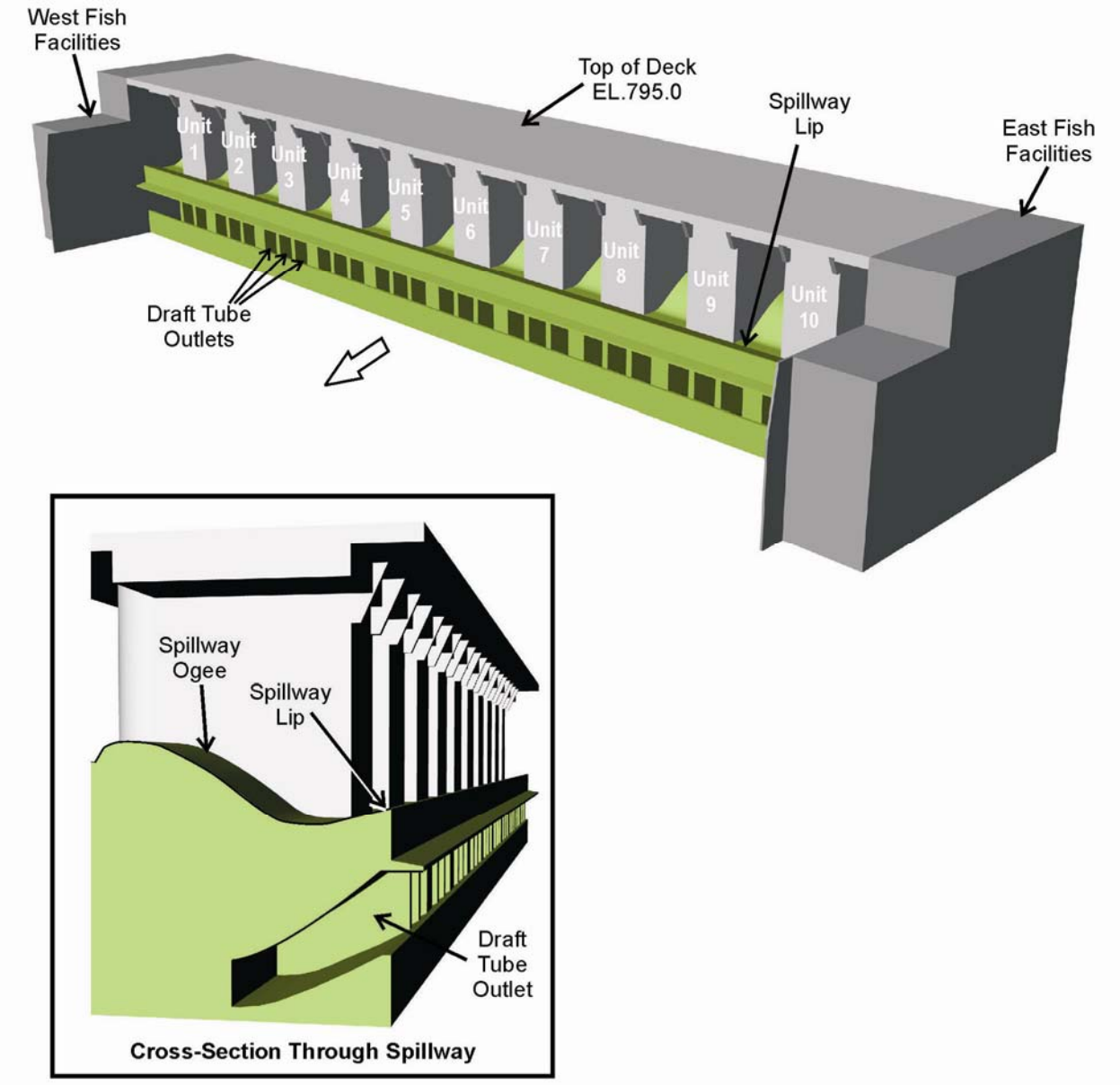

Figure 5.2-1 Structures included in the TDG model

5.3 VOF Model

5.3.1 Mathematical Model

In the VOF model, the interface between fluids is calculated with a water volume fraction (α_w) transport equation:

$$\frac{\partial \alpha_w}{\partial t} + \vec{v} \cdot \nabla \alpha_w = 0 \qquad (1)$$

Mass conservation requires that $\sum \alpha_i = 1$. The jump conditions across the interface are embedded in the model by defining the fluid properties as: $\varphi = \sum \alpha_i \varphi_i$, where φ is either the density or the viscosity. In the VOF approach, each control volume contains just one phase (or the interface). Points in water have $\alpha_w = 1$, points in air have $\alpha_w = 0$, and points near the interface have $0 < \alpha_w < 1$. The free surface was generally defined in the VOF using an α_w of 0.5.

5.3.2 Grid Generation

The domain was divided into a number of blocks and a structured mesh was generated in each block with common interfaces between the blocks. Each individual block consists of hexahedral cells. To resolve the critical regions of interest, the grids were refined near the solid boundaries, near the turbine intakes and spillway where large accelerations are expected, and near the free surface. The grids containing between 6×10^5 to 8×10^5 nodes were generated using Gridgen V15. Grid quality is an important issue for free surface flow simulations. As fine grids are needed near the interface to minimize numerical diffusion, each simulation required the construction of a particular grid. The grids were constructed nearly orthogonal in the vicinity of the free surface to improve convergence. Figure 5.3-1 shows an overall 3D view of the grid used for the June 5, 2006 simulation. An extra volume at the top of the grid was included to accommodate the air volume for the VOF method.

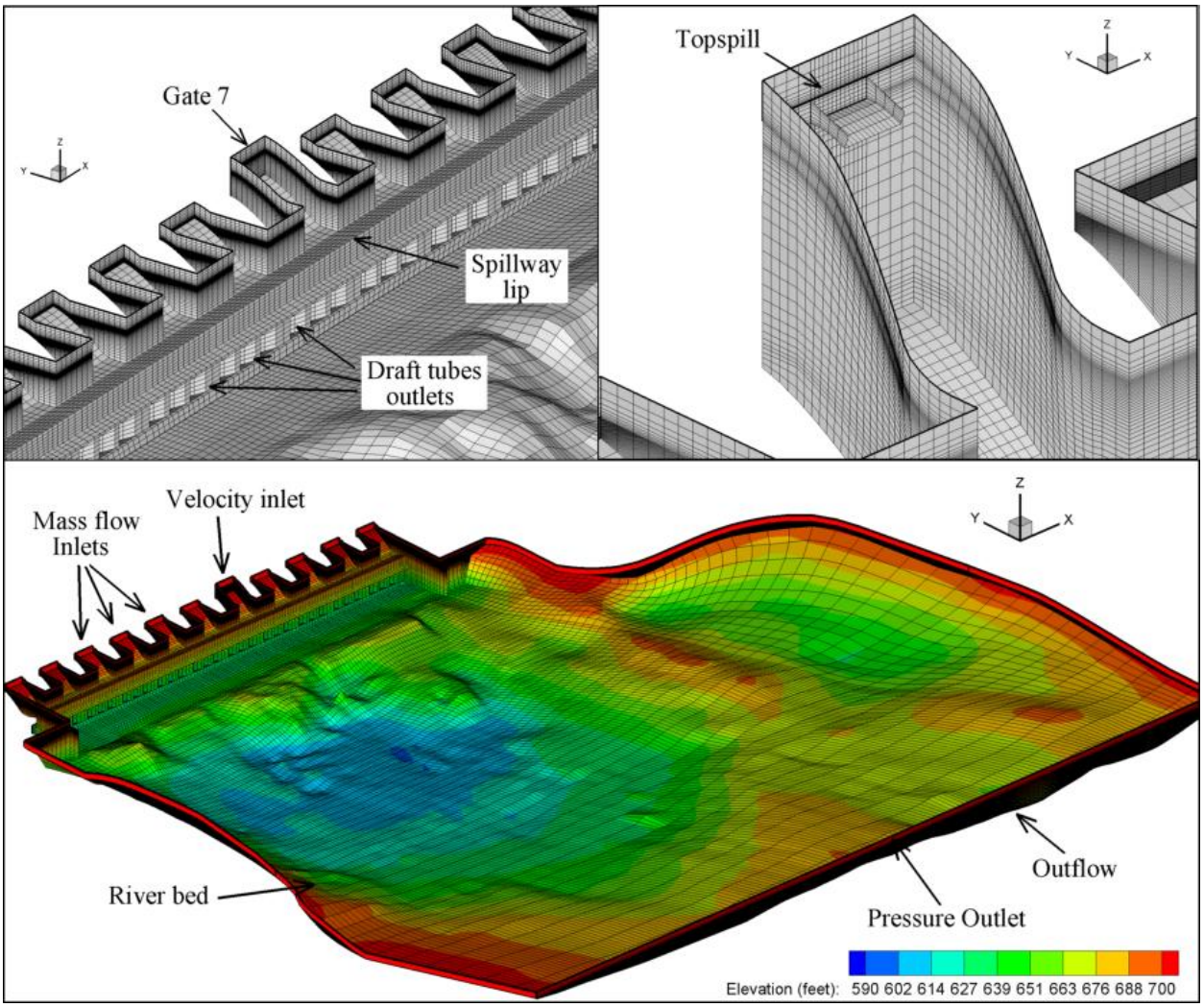

Figure 5.3-1 3D view of a typical grid used for the VOF simulations

5.3.3 Boundary Conditions

5.3.3.1 Inlet

A given mass flow rate of water assuming uniform velocity distribution was used at each of the turbine units and spillway bays.

5.3.3.2 Walls and River Bed

A no-slip (zero velocity) surface condition was imposed on all walls and tailrace bed.

5.3.3.3 Exit

The free water surface elevation (WSE) was imposed by specifying the water volume fraction distribution. The WSE measured at the tailwater elevation gage was used at the exit (outflow

condition in Figure 5.3-1). A hydrostatic pressure was imposed at the outflow using a UDF. At the top of the outflow a pressure outlet boundary condition was used to avoid air pressurization.

5.3.3.4 Top Surface

A pressure outlet boundary condition with atmospheric pressure was applied at the top to allow free air flow and avoid unrealistic pressure.

5.4 Rigid-lid Model

The rigid-lid model is an algebraic slip mixture model (ASMM) (Mannheim et al. 1997) that accounts for buoyancy, pressure, drag and turbulent dispersion forces to calculate the gas volume fraction and velocity of the bubbles. The model considers the change of the effective buoyancy and viscosity caused by the presence of the bubbles on the liquid and the forces on the liquid phase due to the non-zero relative bubble-liquid slip velocity.

5.4.1 Mathematical Model

5.4.1.1 Mass and Momentum Conservation for the Mixture

The two phase model provides mass and momentum equations for the liquid and gas phases (Drew & Passman 1998). Summing the mass and momentum equations for each phase results in continuity and momentum equations for the mixture gas-liquid phase:

$$\frac{\partial \rho_m}{\partial t} + \nabla \cdot \left[\rho_m \, \vec{u}_m \right] = 0 \tag{2}$$

$$\frac{\partial}{\partial t}\left(\rho_m \, \vec{u}_m \right) + \nabla \cdot \left(\rho_m \, \vec{u}_m \, \vec{u}_m \right) = -\nabla P + \nabla \cdot \left[\boldsymbol{\sigma}_m^{\mathrm{Re}} + \boldsymbol{\tau}_m \right] + \rho_m \, \vec{g} - \nabla \cdot \left(\sum_{k=g,l} \alpha_k \, \rho_k \, \vec{u}_k \, \vec{u}_{dr,k} \right) \tag{3}$$

where P is the total pressure, $\vec{g}$ is the gravity acceleration, and $\boldsymbol{\sigma}_m^{\mathrm{Re}}$ and $\boldsymbol{\tau}_m = \rho_m \nu_m \left(\nabla \vec{u}_m + \nabla \vec{u}_m^T \right)$ are the turbulent and molecular shear stresses, respectively. ρ_m, μ_m and $\vec{u}_m$ are the mixture density, viscosity and mass-averaged velocity defined as $\rho_m = \sum_{k=g,l} \alpha_k \, \rho_k$, $\mu_m = \sum_{k=g,l} \alpha_k \, \mu_g$ and $\vec{u}_m = \frac{1}{\rho_m} \sum_{k=g,l} \alpha_k \, \rho_k \, \vec{u}_k$, with α_g the gas volume fraction. The subscripts *g, l* and *m* denote gas, liquid and mixture, respectively. $\vec{u}_{dr,k}$ is the drift velocity defined as the velocity of the phase k relative to the mixture velocity.

The gas density is calculated using the ideal gas law $\rho_g = M \, P / \left(RT \right)$ with P the pressure, M the molecular weight of air, R the universal gas constant, and T the absolute temperature.

5.4.1.2 Mass Conservation for the Gas Phase

The continuity equation for the gas phase is (Drew & Passman, 1998):

$$\frac{\partial}{\partial t}\left(\alpha_g \rho_g\right) + \nabla \cdot \left(\alpha_g \rho_g U_{g,i}\right) = -S \tag{4}$$

where $\vec{u}_g$ is the bubble velocity and S is a negative gas mass source; in this application the TDG source due to the air transfer from the bubbles to the liquid.

5.4.1.3 Momentum Conservation for the Gas Phase

The ASMM assumes that the inertia and viscous shear stresses are negligible compared to pressure, body forces and interfacial forces in the momentum equation of the gas phase (Antal et al., 1991; Lopez de Bertodano et al., 1994; Manninen et al., 1997):

$$0 = -\alpha_g \nabla P + \alpha_g \rho_g \vec{g} + \vec{M}_g \tag{5}$$

where $\vec{M}_g$ represents the interfacial momentum transfer between the phases.

5.4.1.4 Bubble Number Density Transport Equation

Most of the two fluid models in commercial codes (Fluent, CFX, CFDLib, among others) assume a mean constant bubble size with a given relative velocity (Chen et al., 2005). In tailrace flows the use of a mean constant bubble size for the evaluation of the bubble-liquid mass transfer and interfacial forces is not valid. As a consequence of the complex processes of generation, breakup, and coalescence, the bubbles resulting from air entrainment have different sizes. These processes occur at the plunging jet region immediately after the spillway, where the gas volume fraction and turbulence can be large. The model used in this study is intended for the region downstream of the plunging jet, where bubble size changes mainly due to mass transfer and pressure variations, and therefore bubble breakup and coalescence processes can be neglected. This assumption is considered a reasonable hypothesis for low gas volume fractions (Politano et al. 2007).

Let $f\, dm\, d\vec{r}$ represent the number of bubbles with original (at the insertion point, before any physical process modifies the bubble mass) mass m, located within $d\vec{r}$ of $\vec{r}$ at time t. The Boltzmann transport equation for f is:

$$\frac{\partial f}{\partial t} + \nabla \cdot \left[\vec{u}_g\, f\right] + \frac{\partial}{\partial m}\left[\frac{\partial m}{\partial t} f\right] = 0 \tag{6}$$

Note that this is a Lagrangian representation, and thus f has a different interpretation than the usual Eulerian approach (Guido-Lavalle et al., 1994; Politano et al., 2000). Integration of Eq. (6) for bubbles of all masses results in a transport equation for the bubble number density N :

$$\frac{\partial N}{\partial t} + \nabla \cdot \left[\vec{u}_g \, N \right] = 0 \tag{7}$$

The bubble radius is calculated from $R = \left[3\alpha / (4\pi N) \right]^{1/3}$.

5.4.1.5 Two-phase TDG Transport Equation

TDG is calculated with a two-phase transport equation (Politano et al. 2007):

$$\frac{\partial \alpha_l C}{\partial t} + \nabla \cdot \left(\vec{u}_l \, \alpha_l \, C \right) = \nabla \cdot \left(\left(\nu_m + \frac{\nu_t}{Sc_C} \right) \alpha_l \nabla C \right) + S \tag{8}$$

where C is the TDG concentration, and ν_m and ν_t are the molecular and turbulent kinematic viscosity, respectively. In this study, a standard Schmidt number of $Sc_C = 0.83$ is used.

5.4.1.6 Turbulence Closure

In this study a Reynolds Stress Model (RSM) was used. The ASMM assumes that the phases share the same turbulence field. The turbulence in the mixture phase is computed using the transport equations for a single phase but with properties and velocity of the mixture. The transport equations for the Reynolds stresses $\boldsymbol{\sigma}_{i,j}^{\mathrm{Re}} = \rho_m \overline{u'_{m,i} \, u'_{m,j}}$ are:

$$\frac{\partial \boldsymbol{\sigma}^{\mathrm{Re}}}{\partial t} + \left(\nabla \cdot \vec{u}_m \right) \boldsymbol{\sigma}^{\mathrm{Re}} + \vec{u}_m \left(\nabla \cdot \boldsymbol{\sigma}^{\mathrm{Re}} \right) = \nabla \cdot \left[\rho_m \frac{\nu_m^t}{\sigma_R} \nabla \boldsymbol{\sigma}^{\mathrm{Re}} \right] - \mathbf{P} + \boldsymbol{\varphi} + \boldsymbol{\varepsilon} + \mathbf{S}_{\boldsymbol{\sigma}} \tag{9}$$

where the stress production tensor is given by $\mathbf{P} = \boldsymbol{\sigma}^{\mathrm{Re}} \cdot \nabla \vec{u}_m^T + \left(\boldsymbol{\sigma}^{\mathrm{Re}} \cdot \nabla \vec{u}_m^T \right)^T$, $\boldsymbol{\varepsilon} = 2/3 \, \mathbf{I} \, \rho_m \, \varepsilon$ and $\sigma_R = 0.85$. The pressure-strain tensor $\boldsymbol{\varphi}$ is calculated using the models proposed by Gibson and Lander (1978), Fu et al. (1987) and Launder (1989). In this study, $\mathbf{S}_{\boldsymbol{\sigma}}$ represents the effect of the bubbles on the Reynolds stresses. The transport equation for the turbulent dissipation rate reads:

$$\frac{\partial}{\partial t} \left(\rho_m \, \varepsilon \right) + \nabla \cdot \left(\rho_m \, \vec{u}_m \, \varepsilon \right) = \nabla \cdot \left[\rho_m \left(\nu_m + \frac{\nu_m^t}{\sigma_\varepsilon} \right) \nabla \varepsilon \right] - C_{\varepsilon 1} \, \rho_m \, \frac{1}{2} \mathrm{Tr}\left(\mathbf{P} \right) \frac{\varepsilon}{k} - C_{\varepsilon 2} \, \rho_m \frac{\varepsilon^2}{k} + S_\varepsilon \tag{10}$$

with $C_{\varepsilon 1} = 1.44$, $C_{\varepsilon 2} = 1.92$, and $\sigma_\varepsilon = 1$. The turbulent kinetic energy is defined as $k = \frac{1}{2 \rho_m} \mathrm{Tr}\left(\boldsymbol{\sigma} \right)$. The source term S_ε accounts for the effect of the bubbles on the turbulent

dissipation rate. The turbulent kinematic viscosity is computed as in the $k-\varepsilon$ models using $\nu_t = C_\mu k^2/\varepsilon$, with $C_\mu = 0.09$.

5.4.1.7 Constitutive Equations

In order to close the model, interfacial transfer terms emerging from the relative motion between the bubbles and the continuous liquid need to be modeled.

Interfacial momentum

Since in this particular application there are no significant velocity gradients or flow accelerations (in the bubble scale), most interfacial forces such as lift and virtual mass are negligible compared with drag and turbulent dispersion forces:

$$\vec{M}_g = \vec{M}_g^D + \vec{M}_g^{TD} \tag{11}$$

where $\vec{M}_g^D$ and $\vec{M}_g^{TD}$ are the drag and turbulent dispersion terms. The drag force can be modeled as (Ishii & Zuber, 1979):

$$\vec{M}_g^D = -\frac{3}{8}\rho_m \alpha_g \frac{C^D}{R}\vec{u}_r|\vec{u}_r| \tag{12}$$

where $\vec{u}_r$ is the relative velocity of the gas phase respect to the liquid phase. Most of the numerical studies use drag correlations based on rising bubbles through a stagnant liquid proposed by Ishii & Zuber (1979) (see Lane et al., 2005):

$$C^D = \begin{cases} \dfrac{24}{\mathrm{Re}_b} & if\ R < 0.002 \\ \dfrac{24\left(1+0.15\,\mathrm{Re}_b^{0.867}\right)}{\mathrm{Re}_b} & if\ 0.002 < R < 0.00222 \\ 0.56 & if\ R > 0.00222 \end{cases} \tag{13}$$

where $\mathrm{Re}_b = 2\rho_l|\vec{u}_r|R/\mu_l$ is the bubble Reynolds number. The turbulent dispersion term is modeled as (Carrica et al., 1999):

$$\vec{M}_g^{TD} = -\frac{3}{8}\frac{\nu^t}{Sc_b}\rho_m \frac{C^D}{R}|\vec{u}_r|\nabla\alpha_g \tag{14}$$

where $Sc_b = \nu^t / \nu^b$ is the bubble Schmidt number. Following Carrica et al. (1999), $Sc_b = 1$ is used.

Bubble dissolution and absorption

The rate of mass transfer is computed considering that the air is soluble in water and obeys Henry's law and that the air molar composition is that of equilibrium at atmospheric pressure, which implies that the air is considered a single gas with molar averaged properties. The mass flux from gas to liquid can be expressed by (Deckwer 1992; Politano et al. 2007):

$$S = 4\pi N R^2 k_l \left(\frac{P + \sigma/R}{He} - C \right) \tag{15}$$

where σ is the interfacial tension and He is the Henry constant. The second term on the RHS of Eq. (15) accounts for the effect of the interfacial tension on the equilibrium concentration. Takemura and Yabe (1998) proposed a correlation for the mass transfer coefficient of spherical rising bubbles, where the turbulence is generated by the rising bubbles:

$$k_l^{rb} = \frac{D\, Pe_b^{0.5}}{\sqrt{\pi} R} \left(1 - \frac{2}{3\left(1 + 0.09\, \mathrm{Re}_b^{2/3}\right)^{0.75}} \right) \tag{16}$$

where D is the molecular diffusivity and the bubble Peclet number is $Pe_b = 2 \left| \overrightarrow{u_r} \right| R / D$.

External turbulence could be important in flows downstream of spillways, mainly in regions of high shear near the walls and where the plunging jet impacts and enhances the mass transfer. In this application, the mass transfer coefficient can be calculated using the expression proposed by Lamont and Scott (1970):

$$k_l^t = 0.4\, Sc^{-1/2} (\nu \varepsilon)^{1/4} \tag{17}$$

where $Sc = D/\nu$. In this study, the same order of magnitude is obtained from Eqs. (16) and (17), thus the maximum mass transfer coefficient between bubbles rising in stagnant liquid (k_l^{rb}) and bubbles in turbulent flow (k_l^t) is used: $k_l = \max\left(k_l^{rb}, k_l^t\right)$.

5.4.2 Grid Generation

The Wells tailrace structures and the bathymetry are meshed with structured and unstructured multi-block grids containing only hexahedral elements, using Gambit and Gridgen V15. Typical grid sizes are in the range of 7 10^5 to 1 10^6 nodes. Figure 5.4-1 shows typical grids used for the rigid-lid model. Details (a) and (b) show free surface shapes for spread and concentrated flows, respectively. Detail (c) shows the unstructured grid, extended from approximately 1,500 feet to 3,500 feet downstream of the Wells Dam, used to reduce grid size and improve aspect ratio.

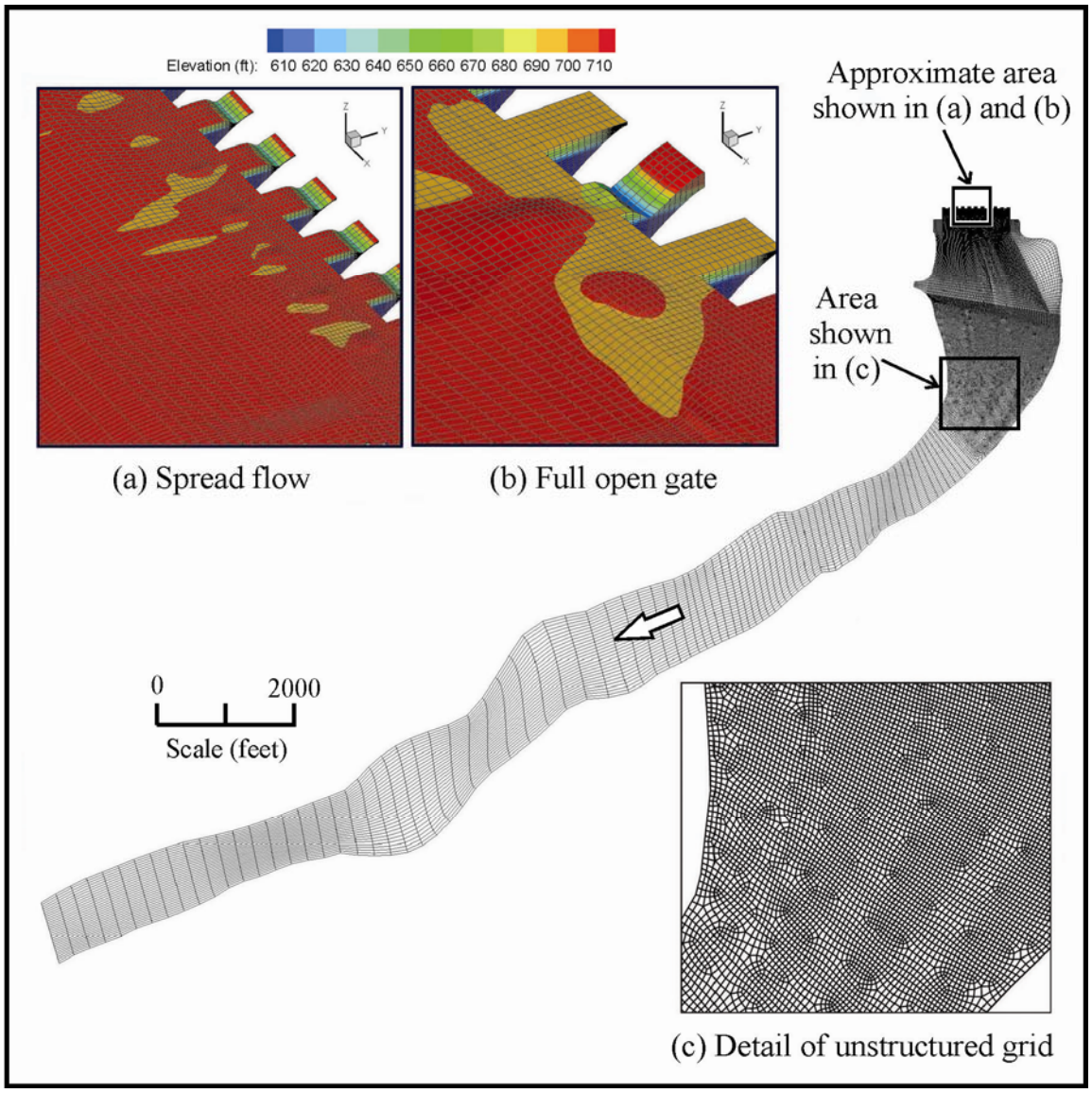

Figure 5.4-1 3D view of a typical grid used for the rigid-lid simulations

5.4.3 Boundary Conditions

5.4.3.1 Free Surface

Kinematic and dynamic boundary conditions enforcing zero normal velocity fluctuations at the free surface are programmed through UDFs. Details of the implementation of the boundary conditions used for the Reynolds stress and velocity components are found in Turan et al. (2007).

In order to allow the gas phase to flow across the interface, the normal component of the gas velocity at the free surface is calculated using a mass balance for the gas phase in each control volume contiguous to the interface. The resulting equation is implemented using UDFs.

For the TDG concentration, a Neumann boundary condition is used. A mass transfer coefficient at the free surface of $k_l = 0.0001$ m/s as measured by DeMoyer et al. (2003) for tanks and bubble columns is used.

5.4.3.2 Walls and River Bed

The sides and the river bed are considered impermeable walls with zero TDG flux. For the gas phase, no penetration across walls is imposed.

5.4.3.3 Exit

The river exit is defined as an outflow. A zero gradient condition was programmed for the TDG concentration and bubble number density.

5.4.3.4 Spillbays and Powerhouse Units

Uniform velocities with constant gas volume fraction of $\alpha = 0.03$ and bubble diameter 5 mm are used for the 11 bays in the spillway region.

It is assumed that air is not entrained with the turbine inflow. The TDG concentration measured in the forebay is used at the spillway bays and powerhouse units.

6.0 RESULTS

The computations were performed using 4 processors of a Linux cluster with 2 Gb of memory per processor and in three dual socket dual core Xeon Mac Pro systems.

6.1 VOF Model

The discrete RANS equations and Eq. (1) were solved sequentially (the segregated option in Fluent) and coupled to a realizable $k-\varepsilon$ model with wall functions for turbulence closure. The pressure at the faces is obtained using the body force weighted scheme. The continuity equation was enforced using a Semi-Implicit Method for Pressure-Linked (SIMPLE) algorithm. A modified High Resolution Interface Capturing (HRIC) scheme was used to solve the gas volume fraction.

Unsteady solutions were obtained using variable time-step between 0.001 to 0.01 seconds. Typically, two to three nonlinear iterations were needed within each time step to converge all variables to a L_2 norm of the error $<10^{-3}$. The flow rate at the exit and the elevation at the tailwater elevation gauge location were selected as convergence parameters.

6.1.1 Calibration

The calibration cases were run in a domain of approximately 3,000 ft downstream of the dam. Zero velocities and turbulence were used as initial conditions in the entire domain.

The convergence parameters for the calibration cases were:

$$46 S - June\ 4, 2006 \rightarrow \left(flowrate : 172.4, WSE : 717.3\ ft \right)$$

$$47 FG - June\ 5, 2006 \rightarrow \left(flowrate : 222.3, WSE : 720.2\ ft \right)$$

Horizontal lines in Figure 6.1-1 show the target flowrate (blue line) and WSE at the tailwater elevation gage (green line). The evolution of the simulations for the calibration cases is illustrated in Figure 6.1-1; blue lines represent the flow rate at the exit and the green lines the free surface elevation. It was considered that statistically steady solutions were obtained at approximately 30 minutes, which required about 60 days of computation time.

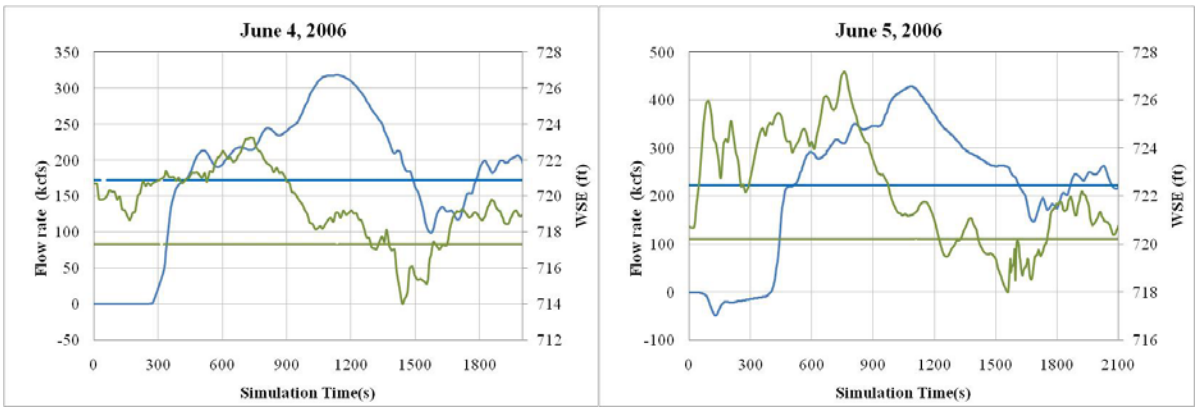

Figure 6.1-1 Evolution of the flowrate at the exit (blue line) and free surface elevation (green line) for June 4, 2006 and June 5, 2006. Horizontal lines represent target values.

Figure 6.1-2 shows an isosurface of gas volume fraction $\alpha_w = 0.5$ representing the free-surface location used to create the top of the rigid-lid grid for the June 4, 2006 simulation. In Figure 6.1-3 a horizontal slice at 27 ft from the free-surface (top) and a vertical section at the center of spillway bay 7 (bottom) show the predicted flow field with the VOF method. Red and blue contours represent water and air, respectively. For clarity, predicted velocity vectors were interpolated in structured uniform grids. Almost uniform flow is observed close to the spillway during the spread flow operation. Surface jets are predicted in all the spillway bays due to elevated tailwater levels. In addition, water flow from the powerhouse units prevented the spillway jet from plunging to depth within the stilling basin.

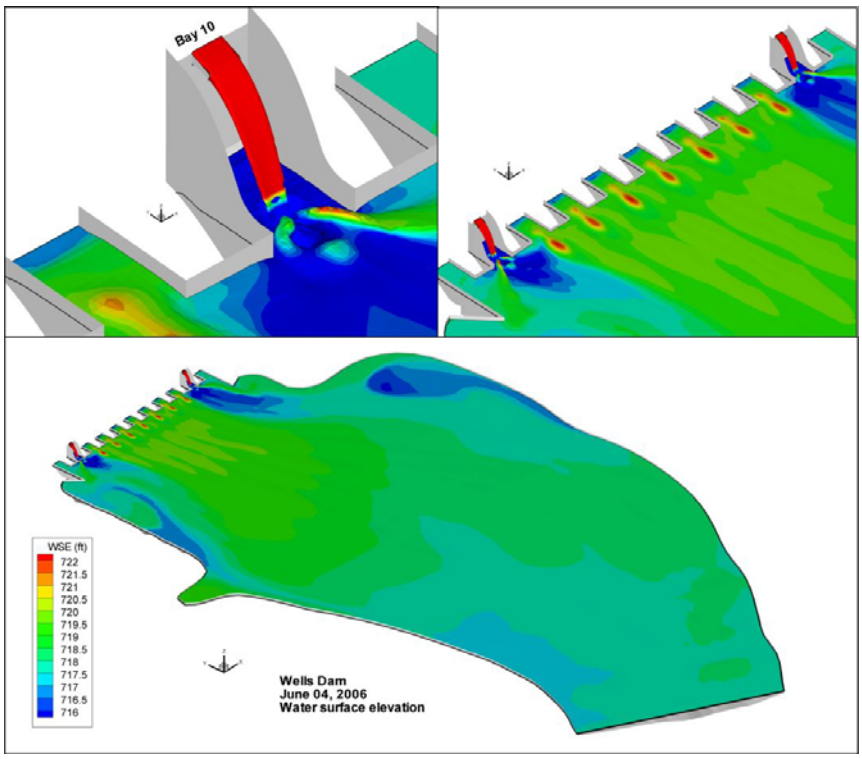

Figure 6.1-2 Predicted free surface shape for June 4, 2006

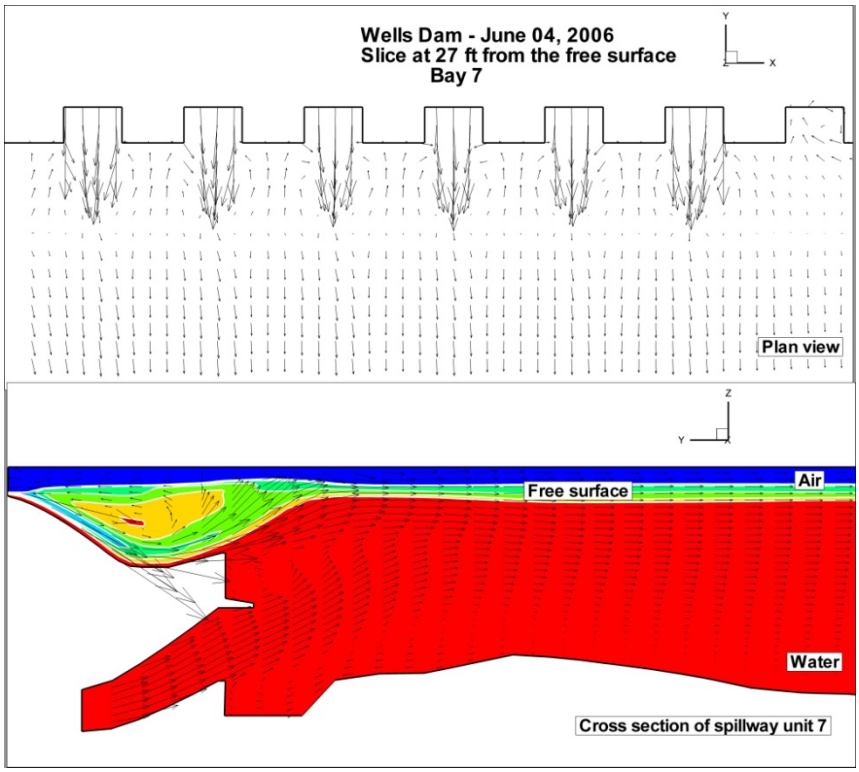

Figure 6.1-3 Predicted flow field for June 4, 2006

The free surface used to create the rigid-lid grid for June 5, 2006 is shown in Figure 6.1-4. The horizontal slice at the top of Figure 6.1-5 shows the water attraction toward the surface jet on bay 7 (water entrainment) caused by the full open gate operation. The water entrainment originates two large eddies near the east and west bank of the Wells tailrace. As observed on June 4, 2006, the strong surface jet originated in bay 7 remains close to the free surface (see bottom picture in Figure 6.1-5) due to the favorable tailwater elevation and plant operation on this day.

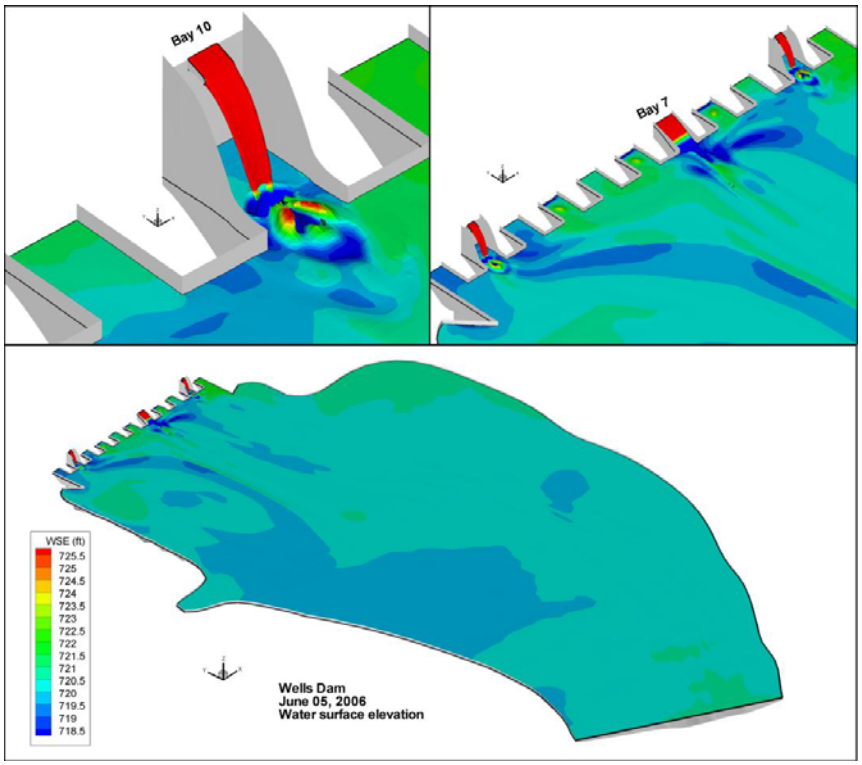

Figure 6.1-4 Predicted free surface shape for June 5, 2006

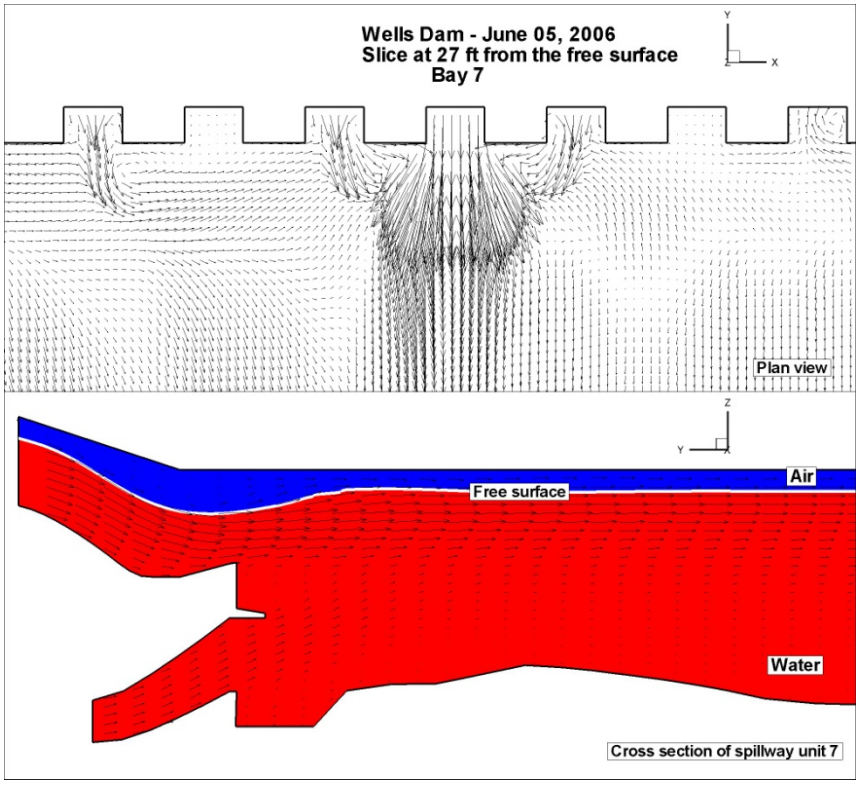

Figure 6.1-5 Predicted flow field for June 5, 2006

6.1.2 Model Validation

The domain used to simulate the validation cases was reduced to 1,700 ft downstream of the dam with the purpose of speeding up the VOF computations. During the calibration it was observed that the effect of the top spill on the free surface shape is limited to a small region near spillway bays 2 and 10. Therefore the validation cases assumed that spillway bays 2 and 10 were closed and the free surface shape obtained during the calibration process was used near the top spills.

The numerical solution (pressure, velocity, free surface location and turbulent quantities) obtained on June 5, 2006 was used as an initial condition for the validation cases.

The convergence parameters for the calibration cases were:

$$1FG - May\ 14, 2006 \rightarrow \left(flowrate : 120.4, WSE : 711.5\ ft \right)$$

$$11FG - May\ 17, 2006 \rightarrow \left(flowrate : 157.2, WSE : 715.4\ ft \right)$$

$$63C - June\ 17, 2006 \rightarrow \left(flowrate : 205.5, WSE : 718.6\ ft \right)$$

Figure 6.1-6 shows the evolution of the flowrate and WSE at the tailwater elevation gauge for the validation cases. Blue and green lines represent the flowrate and WSE, respectively. The above mentioned simplifications allowed the calibration cases to reach the statistically steady solutions in typically 20 minutes using 30 days of computation time.

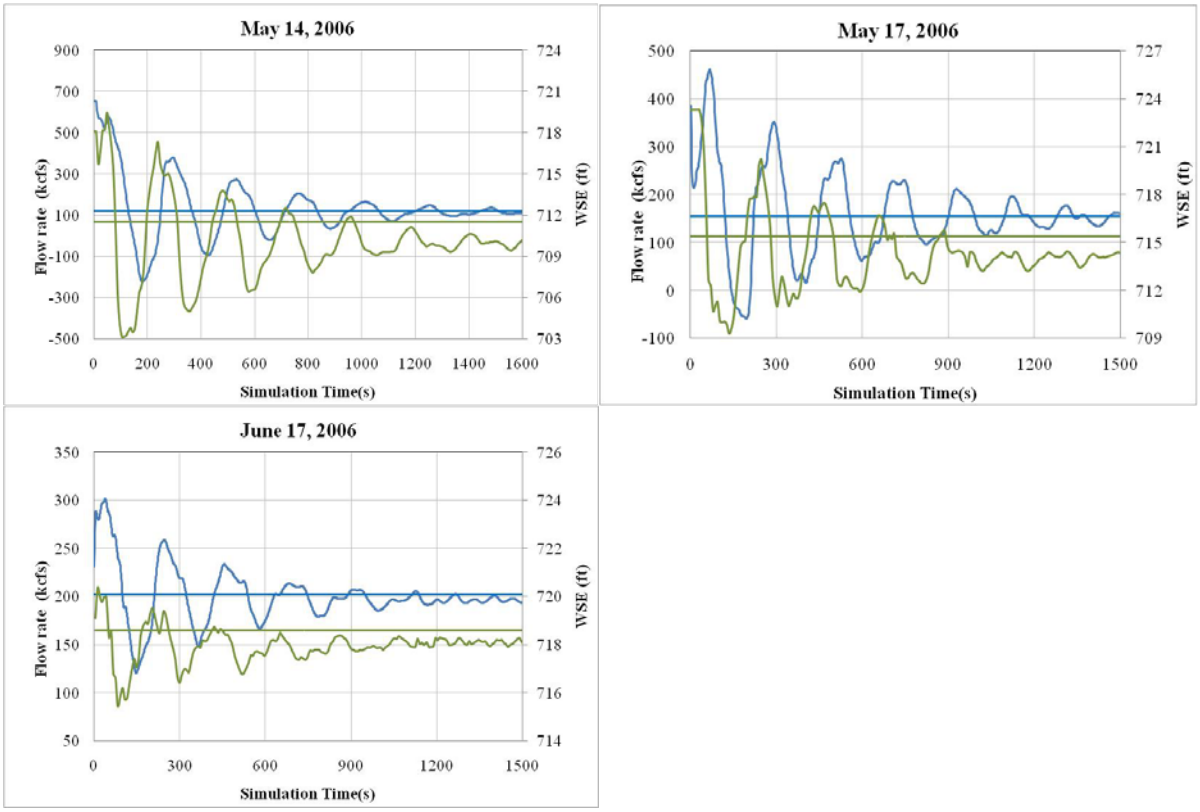

Figure 6.1-6 Evolution of the flowrate at the exit (blue line) and free surface elevation (green line) for May 14, 2006, May 17, 2006, and June 17, 2006. Horizontal lines represent target values.

6.2 Rigid-lid Model

The ASSM model equations were solved sequentially. The VOF and rigid-lid simulations were performed using the same discretization schemes for the continuity and pressure equations. A first order upwind scheme was used for the gas volume fraction and Reynolds stress components.

Unsteady solutions were obtained using a fixed time-step of 10 seconds. In order to improve convergence, the model was first run assuming single-phase flow and then bubbles were injected into the domain. The rigid-lid model was computed in typically 7 hours (2 days of computation time) to obtain a steady condition for the flow field and TDG concentration.

6.2.1 Hydrodynamics

Figures 6.2-1 and 6.2-2 show depth-averaged velocity data collected in the field on June 4, 2006 and June 5, 2006 and those predicted by the rigid-lid model. Good agreement between observed and predicted velocity vectors was found, especially at the downstream transect where flow conditions were more stable and the Acoustic Doppler Current Profiler (ADCP) velocity data are less affected by turbulence and non-steady conditions.

As observed in the field, the model captured the counterclockwise eddy near the east bank and the almost uniform profile at the most downstream transect.

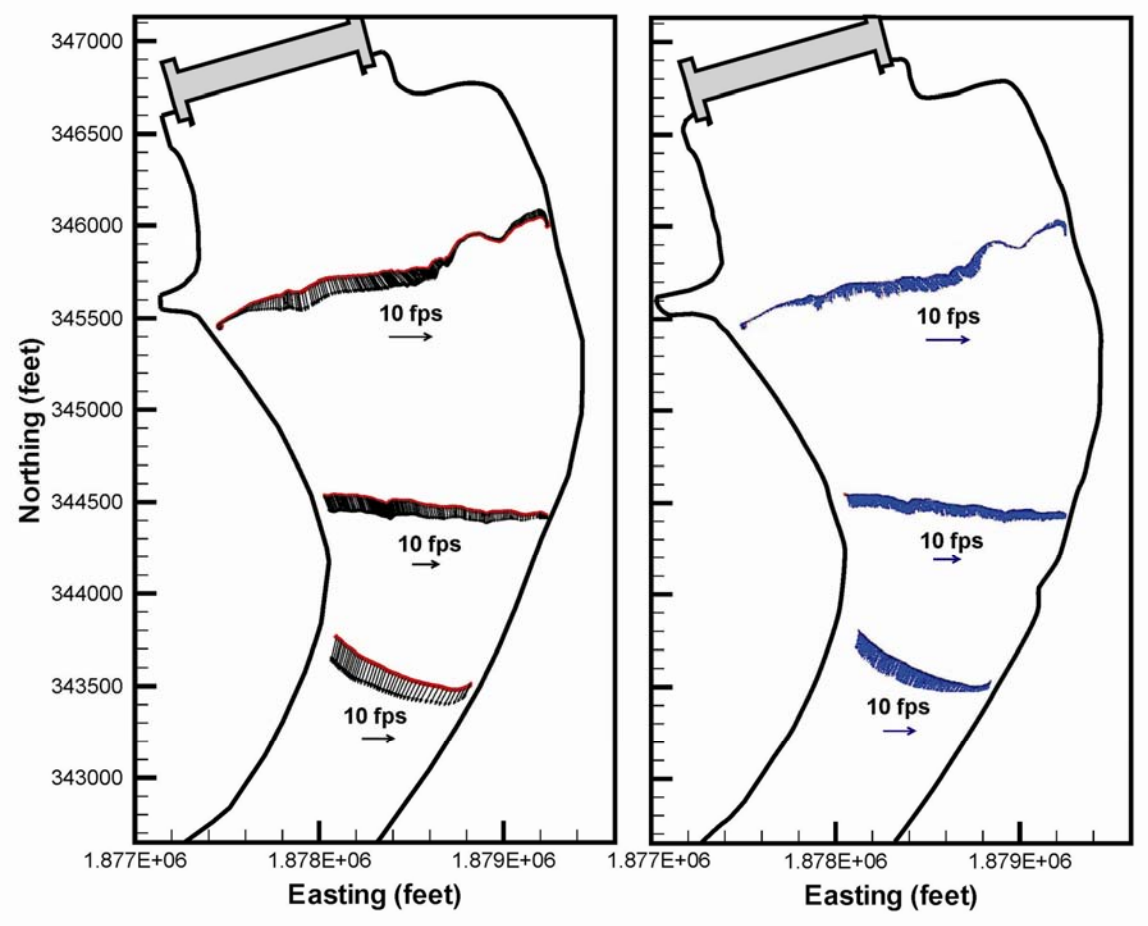

Figure 6.2-1 Flow field on June 4, 2006. Black vectors: rigid-lid model predictions and blue vectors: velocity field data

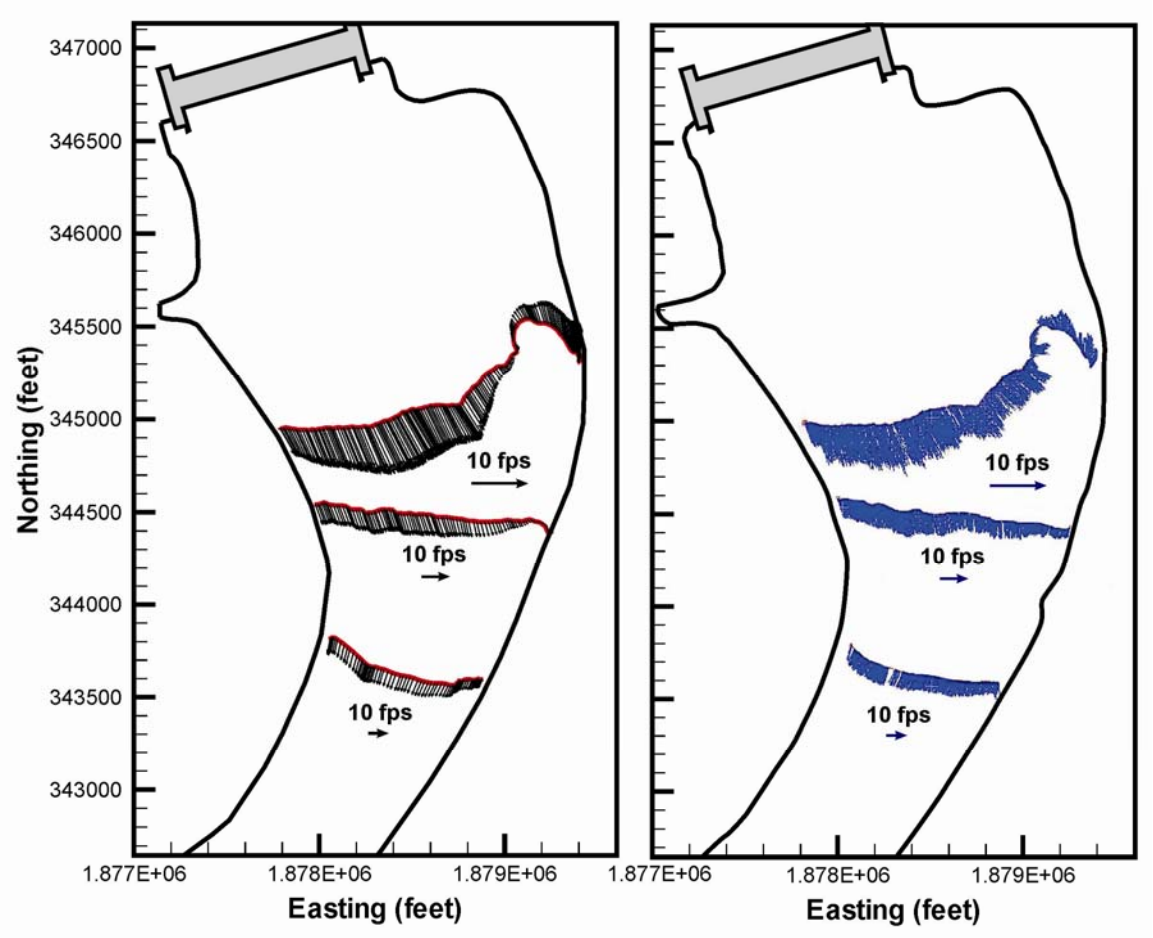

Figure 6.2-2 Flow field on June 5, 2006. Black vectors: rigid-lid model predictions and blue vectors: velocity field data

6.2.2 TDG Model

The percent saturation of TDG measured in the field at each station and the mean TDG in each of the three transects together with the values generated by the CFD model for the calibration and validation cases are shown in Appendix A. Figures 6.2-3 to 6.2-7 show measured and predicted values at each probe location. A bubble diameter of 0.5 mm and gas volume fraction of 3% in the spillbays produced TDG values that bracketed field observations.

The model captures the reduction of TDG with distance downstream and the lateral gradient observed in the field. As measured, the highest predicted TDG value at Transect TW1 occurred in the center of the channel and the lateral gradients in transects TW2 and TW3 were negligible.

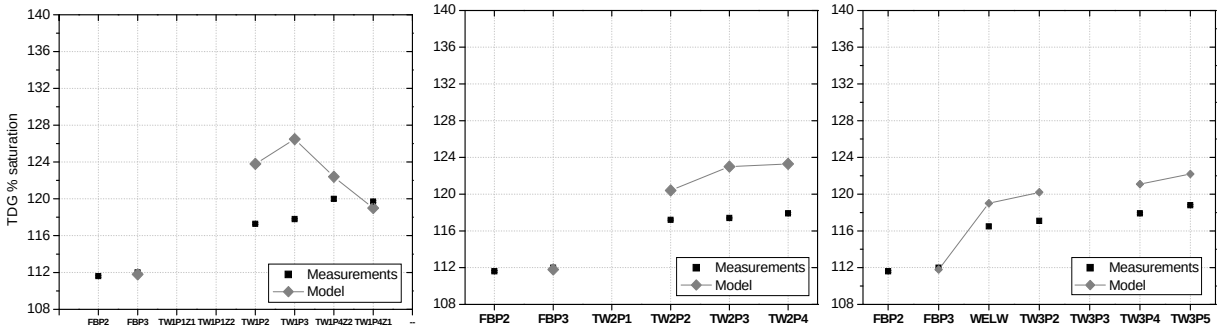

Figure 6.2-3 Comparison between measured and predicted TDG on June 4, 2006. Gray diamonds represent TDG model predictions and black squares represent field observations.

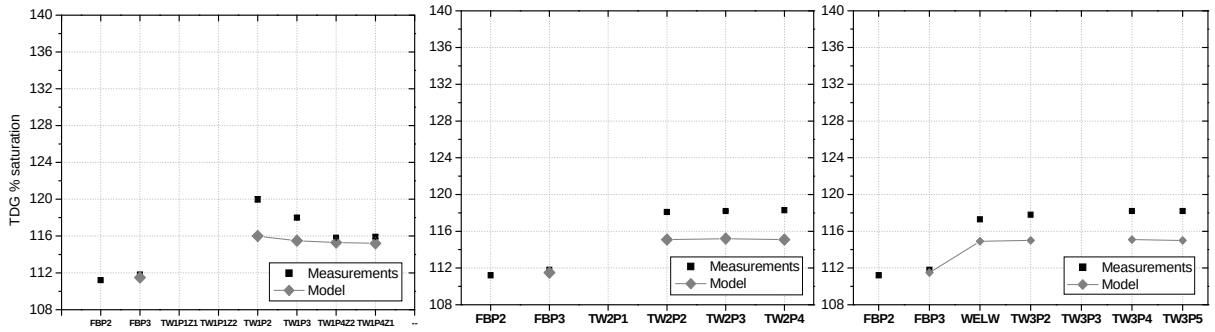

Figure 6.2-4 Comparison between measured and predicted TDG on June 5, 2006. Gray diamonds represent TDG model predictions and black squares represent field observations.

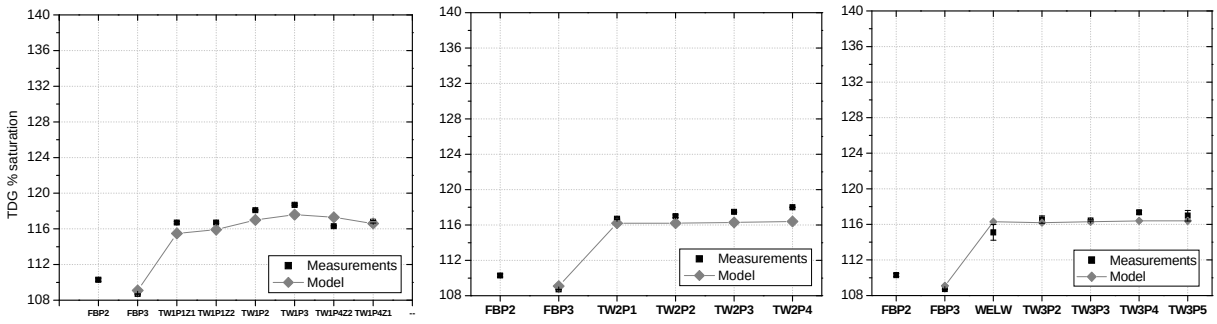

Figure 6.2-5 Comparison between measured and predicted TDG on May 14, 2006. Gray diamonds represent TDG model predictions and black squares represent field observations.

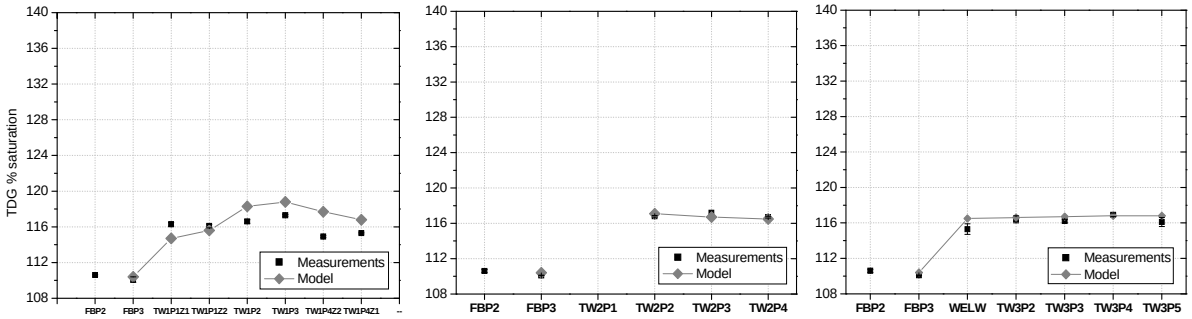

Figure 6.2-6 Comparison between measured and predicted TDG on May 17, 2006. Gray diamonds represent TDG model predictions and black squares represent field observations.

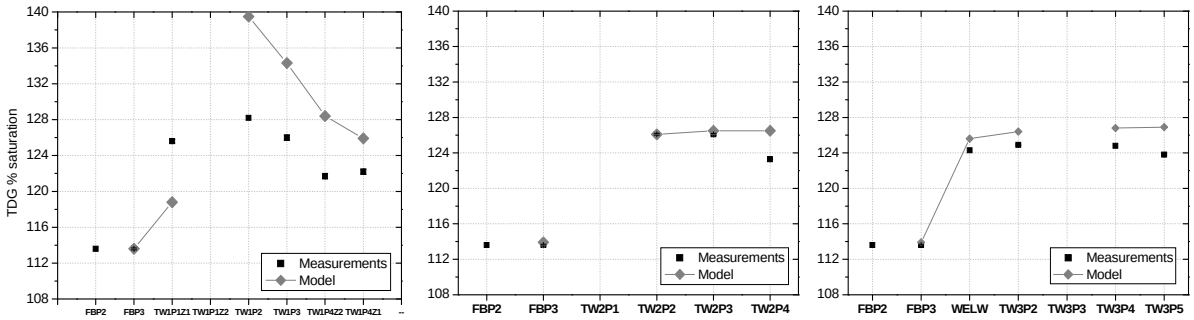

Figure 6.2-7 Comparison between measured and predicted TDG on June 17, 2006. Gray diamonds represent TDG model predictions and black squares represent field observations.

Figures 6.2-8 and 6.2-9 show isosurfaces of TDG, gas volume fraction and bubble diameter for June 4, 2006 and June 5, 2006 where the spill operation of the dam was spread and full open gate, respectively. As shown by the gas volume fraction isosurfaces, the model predicts uniformly distributed bubbles on the spillway region during spread spill operations. On the other hand, bubbles concentrate near the center of the spillway for full open gate operation. The maximum TDG occurs at the center region due to the exposure of water to the aerated flow as it travels within the stilling basin (see TDG isosurfaces). The rate of mass exchange depends on the gas volume fraction, the bubble size and the difference in concentration between the bubble boundary and the water. The gas dissolution region occurs mainly within 500 to 1,000 ft downstream of the spillway; afterwards the bubbles moved up to regions of lower pressure and the dissolution rate decreased. The bubbles shrink near the bed due to the air mass transfer and high pressure. The smaller the bubble size the stronger its tendency to dissolve. Substantial desorption of TDG takes place near the free surface downstream of the spillway. Once the air bubbles are vented back into the atmosphere the rate of mass exchange decreases significantly. The TDG concentration reaches a developed condition approximately 1,300 ft from the spillway. According to the simulation results, the draft tube deck extensions, which tend to act as deflectors for the spill, and powerhouse operation prevented spilled flow from plunging deep, reducing the exposure of bubbles to high pressure.

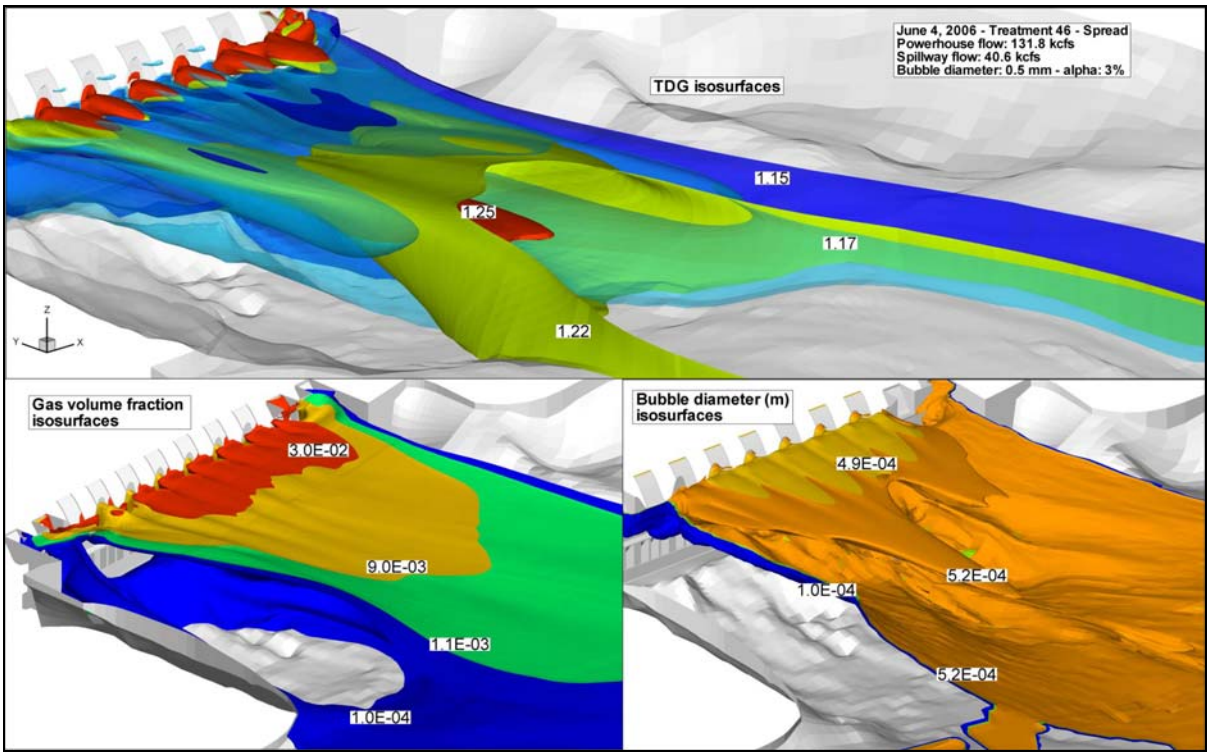

Figure 6.2-8 **TDG, gas volume fraction and bubble diameter isosurfaces for June 4, 2006**

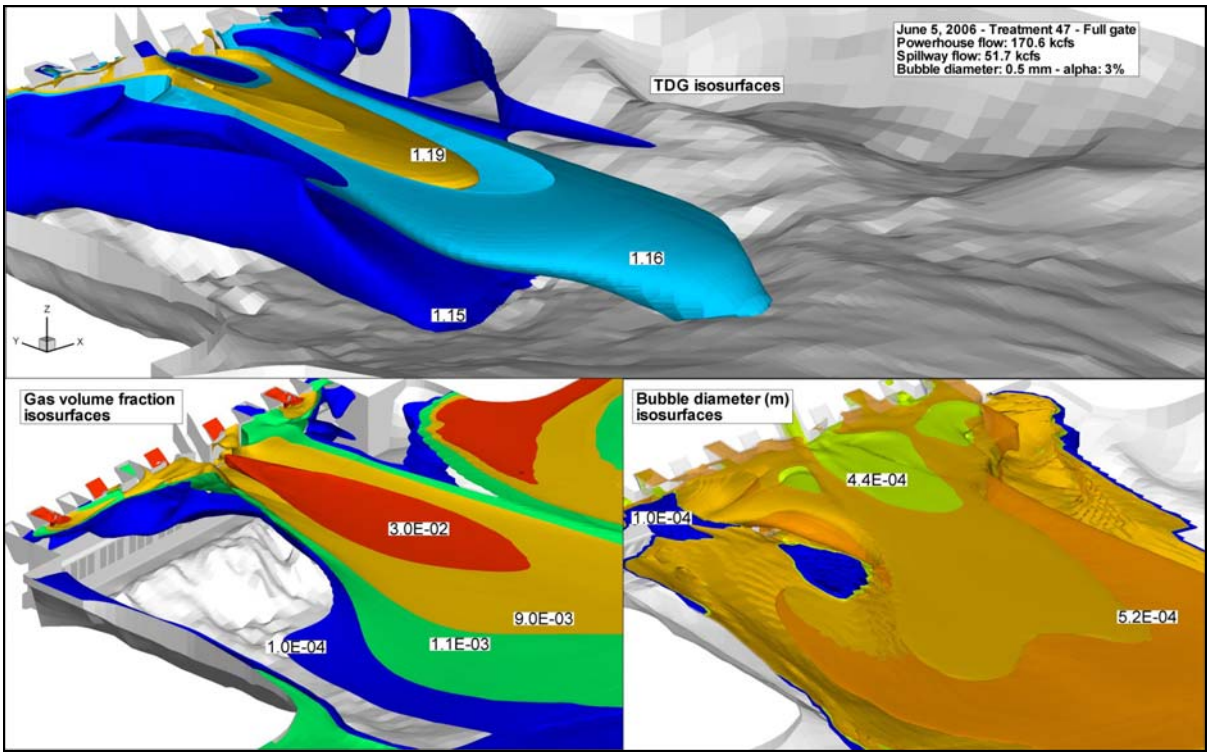

Figure 6.2-9 **TDG, gas volume fraction and bubble diameter isosurfaces for June 5, 2006**

7.0 DISCUSSION

A mixture two-phase flow model aimed at the prediction of TDG in the Wells tailrace was developed. Variable bubble size and gas volume fraction were used to analyze dissolution and the consequent source of TDG. The model uses an anisotropic RSM turbulence model.

The model was calibrated and validated using field data collected on May 14, May 17, June 4 June 5 and June 17, 2006 during the TDG Production Dynamics Study (EES et al., 2007). The spillway flow was spread across spillbays on June 4, concentrated through a single spillbay on May 17, June 4 and June 5, and crowned on June 17. The observed flow field in the tailrace on June 4 and June 5 was properly predicted by the model. The bubble size and gas volume fraction at the inlet were the parameters of the model. A bubble diameter of 0.5 mm and gas volume fraction of 3% in the spillbays produced TDG values that bracketed field observations.

The model captured the lateral TDG distribution and the reduction of TDG longitudinally as observed in the field. The model brackets the results of the field measurements for the validation cases with a deviation of about +/- 3% of the average TDG values for Transect 3. A reasonable evaluation of the model predictability and selection of the best parameters is complicated since the accuracy of the field data is not provided in the field study (EES et al., 2007). The model used in this study assumes that bubble size changes mainly due to mass transfer and pressure and considers that breakup and coalescence are negligible. This hypothesis is frequently used for low volume fraction flows. In this study, the gas volume fraction and bubble size were selected to be above and below the averaged TDG measured on June 4 and 5, 2006. It is expected that the inclusion of the breakup and coalescence phenomena change the bubble size distribution at the plunging jet region immediately downstream of the spillway. However, as the bubble size at the inlet was selected to bracket the field data, breakup and coalescence should play a minor role on the TDG distribution and production in the Wells tailrace.

Possible efforts to further improve the predictive capability of the model include:

- The model assumes that the bubble size and gas volume fraction are the same at the inlet (spillway bay gates) irrespective of spillway operation. The VOF simulations seem to indicate that the flow regime and bubble entrainment in the near field of the plungers are substantially different for spread and full open gate operations. The best agreement is for the full open gate cases. The gas volume fraction (or bubble size) at the inlet could be slightly different for the spread and crown operation. Preliminary sensitivity analyses indicate that a change in the volume fraction from 3% to 4% (or 0.1 mm in bubble diameter) at the inlet could considerably improve the model predictions for spread and crowned operations.
- The incorporation of a temperature model considering the change of the solubility with the temperature. This could capture the TDG fluctuations due to seasonal thermal cycles.
- Bubbles change chemical composition as they dissolved due to the different solubilities of the air components. In this study, the air is considered a unique gas with molar averaged properties. The incorporation of a multi-component model that takes into account the different solubilities of oxygen and nitrogen and therefore

considers the different chemical composition of the bubbles as they transfer mass is proposed as future improvement of the model.

The analysis presented herein seems to indicate that properly modeling the air entrainment boundary condition is the most important improvement to the model at this stage.

In spite of the air entrainment boundary condition uncertainties, this study has demonstrated that the presented model can capture the main features of the two-phase flow in the Wells tailrace and the general trends of TDG values across the transects.

Future work:

With some additional minor adjustments the model described above will be used as a predictive numerical tool to identify Project operations that can be used to minimize TDG concentration downstream of the Wells Project.

The next phases of this study will be executed in two testing stages; Phase 1 and Phase 2.

The purpose of the Phase 1 will be to analyze different spill releases and TDG production as a function of flow and tailwater elevation. In this phase the sensitivity of TDG concentration to the operation of the spillway and tailwater elevation will be studied. Nine runs with two spillway configurations (spread and FG) and four total river flows will be simulated.

Nine additional model runs will be completed in Phase 2. Flow conditions and spill scenarios will depend upon the results of Phase 1. However, Phase 2 will involve more realistic scenarios with practical operational condition to assist in the understanding of optimal spill configurations and plan operation in reducing TDG production.

The final results of the Phase 1 and Phase 2 modeling efforts will be the focus of the final report for this study.

8.0 STUDY VARIANCE

There were no variances from the final FERC approved study plan for the Total Dissolved Gas Investigation. The final study report will be complete and available to the public in early 2009.

9.0 ACKNOWLEDGMENTS

This numerical study was sponsored by Douglas PUD. The authors thank Shane Bickford and Bao Le for their support and cooperation to this study. The constructive suggestions of Duncan Hay of Oakwood Consulting Inc. are gratefully appreciated.

10.0 REFERENCES

Antal, S.P., R.T. Lahey Jr., and J.E. Flaherty. 1991. Analysis of Phase Distribution in Fully Developed Laminar Bubbly Two-Phase Flow, International Journal of Multiphase Flow. 17(5): 553-682

ASL Environmental Sciences Inc. 2007. Turbine discharge measurements by acoustic scintillation flow meter at Until 1 and 2, Wells Hydroelectric Project, Pateros, Washington (2006). Prepared for the Public Utility District No. 1 of Douglas County.

Carrica, P. M., D. Drew, F. Bonetto, and R.T. Lahey Jr. 1999. A Polydisperse model for bubbly two–phase flow around a surface ship. International. Journal of Multiphase Flow. 25: 257-305.

Chen, P., M.P. Dudukovic, and J. Sanyal. 2005. Three-dimensional simulation of bubble column flows with bubble coalescence and breakup. American Institute of Chemical Engineers Journal. 51(3):696-712.

Columbia Basin Environmental (CBE). 2003. Wells Dam Spillway Total Dissolved Gas Evaluation 27 May to 10 June 2003. Final Report. Prepared for Public Utility District No. 1 of Douglas County.

Columbia Basin Environmental (CBE). 2004. Wells Dam Spillway Total Dissolved Gas Evaluation 23 May to 6 June 2004. Final Report. Prepared for Public Utility District No. 1 of Douglas County.

Columbia Basin Environmental (CBE). 2006. Wells Dam Spillway Total Dissolved Gas Evaluation – 23 May to 6 June 2005, Final Report, Prepared for Douglas County PUD.

Douglas County PUD. 2006. Wells Hydroelectric Project. FERC Project No. 2149. Pre-Application Document.

Deckwer, W.D. 1992. Bubble Column Reactors. John Wiley & Sons.

DeMoyer, C.D., E.L. Schierholz, J.S. Gulliver, and S.C.Wilhelms. 2003. Impact of Bubble and Free Surface Oxygen Transfer on Diffused Aeration Systems. Water Research. 37(8):1890-1904.

Drew, D.A., and S.L. Passman. 1998. Theory of Multicomponent Fluids. Applied Mathematical Sciences, Springer 135.

EES Consulting, Inc., J. Carroll, ENSR, and Parametrix. 2007. Total dissolved gas production dynamics Study of the Wells hydroelectric project. Prepared for Public Utility District No. 1 of Douglas County. Kirkland, Washington.

Ferrari, G., M.S. Politano, and L. Weber. 2008. Numerical simulation of free flows on a fish bypass. Computers & Fluids. In press.

Fu, S., B.E. Launder, and D.P. Tselepidakis. 1987. Accommodating the effects of high strain rates in modeling the pressure-strain correlations. The University of Manchester Institute of Science and Technology. TFD/87/5.

Gibson, M.M., and B.E. Launder. 1978. Ground effects on pressure fluctuations in the atmospheric boundary layer. Journal of Fluid Mechanics. 86: 491-511.

Guido-Lavalle, G., P. Carrica, A. Clausse, and M.K. Qazi. 1994. A bubble number density constitutive equation, Nuclear Engineering and Design. 152: 213–224.
Hibbs, D.E., and J.S. Gulliver. 1997. Prediction of Effective Saturation Concentration at Spillway Plunge Pools. Journal of Hydraulic Engineering 123: 940-949.

Ishii, M., and N. Zuber. 1979. Drag Coefficient and Relative Velocity in Bubbly, Droplet or Particulate Flows. American Institute of Chemical Engineers Journal. 25(5):843-855.

Jakobsen, H.A., H. Lindborg, and C.A. Dorao. 2005. Modeling of bubble column reactors: progress and limitations. Industrial & Engineering Chemistry Research 44: 5107-5151.

Klinge, R. 2005. Wells Dam total dissolved gas abatement plan for 2005 and 2006 project. Prepared for Public Utility District No. 1 of Douglas County. East Wenatchee, WA

Lamont, J.C., and D.S. Scott. 1970. An eddy cell model of mass transfer into the surface of a turbulent liquid. The American Institute for Chemical Engineers Journal. 16:513-519.

Lane, G.L., M.P. Schwarz, and G.M. Evans. 2005, Numerical modeling of gas-liquid flow in stirred tanks. Chemical. Engineering. Science. 60: 2203–2214.

Launder, B. E. 1989. Second-moment closure and its use in modeling turbulent industrial flows. International Journal for Numerical Methods in Fluids 9:963-985.

Liepmann, D. 1990. The near-field dynamics and entrainment field of submerged and near surface jets. Ph.D. thesis, University of California, San Diego.

Lopez de Bertodano, M.L., R.T. Lahey Jr, and O.C. Jones. 1994. Development of a $k-\varepsilon$ model for bubbly two-phase flow. Journal of Fluids Engineering. 116: 128-134.

Mannheim, C., and L. Weber. 1997. Hydraulic Model Studies for Fish Diversion at Wanapum/Priest Rapids Development, Part XI: Spillway Deflector Design, Contracted by Public Utility District No. 2 of Grant County, Ephrata, WA. IIHR Limited Distribution Report No. 264.

Orlins, J.J., and J.S. Gulliver. 2000. Dissolved Gas Supersaturation Downstream of a Spillway II: Computational Model. Journal of Hydraulic Engineering 38: 151-159.

Politano, M.S., P.M. Carrica, C. Turan, and L. Weber. 2007a. A multidimensional two-phase flow model for the total dissolved gas downstream of spillways. Journal of Hydraulic Research 45(2): 165-177.

Politano, M.S., C. Turan, P.M. Carrica, and L. Weber. 2007b. A three-dimensional anisotropic model of the two phase flow and total dissolved gas downstream of spillways. FLUCOME.
Politano, M.S., P.M. Carrica, and J.L. Baliño. 2000. A polydisperese model of the two-phase flow in a bubble column. Heat and Technology 18(2): 101-113.

Takemura, F., and A. Yabe. 1998. Gas Dissolution Process of Spherical Rising Gas Bubbles. Chemical Engineering Science. 53(15):2691-2699.

Turan, C., P. M. Carrica, T. Lyons, D. Hay, and L. Weber. 2008. Study of the Free Surface Flow on an Ogee-Crested Fish Bypass. Journal of Hydraulic Engineering. 134: 1172-1175

Turan, C., M.S. Politano, P. M. Carrica, and L. Weber. 2007. Water Entrainment and Mixing due to Surface Jets. Computational Fluid Dynamics, 21: 3-4, 137-153.

Walker, D.T. 1997. On the origin of the 'surface current' in turbulent free-surface flows. Journal of Fluids Engineering 339, 275-285.

Walker, D.T., and C.Y. Chen. 1994. Evaluation of algebraic stress modelling in free-surface jet flows. Journal of Fluids Engineering 118: 48-54

Appendix A

Differences Between Measured and Predicted TDG Concentrations

Comparison between measured and predicted TDG on June 4, 2006

Transect	Easting (feet)	Northing (feet)	Z (feet)	TDG predicted	TDG measured	diff %	Average predicted	Average measured	Average difference (%)
TW1P2	1878138.733	345839.846	648.7	1.238	1.173	5.580			
TW1P3	1877972.651	345812.512	648.4	1.265	1.178	7.41			
TW1P4Z1	1877766.08	345652.528	692.0	1.224	1.200	1.97			
TW1P4Z2	1877685.593	345800.096	657.0	1.190	1.197	-0.61	1.229	1.187	3.56
TW2P2	1878494.473	343593.521	675.9	1.204	1.172	2.72			
TW2P3	1878414.713	343618.277	679.9	1.230	1.174	4.78			
TW2P4	1878237.515	343582.52	698.6	1.233	1.179	4.55	1.222	1.175	4.02
WELW	1870372.891	334581.117	692.0	1.190	1.165	2.18			
TW3P2	1870323.519	334702.235	698.7	1.202	1.171	2.69			
TW3P4	1870037.256	334948.965	673.4	1.211	1.179	2.74			
TW3P5	1869929.689	335169.057	697.9	1.222	1.188	2.87	1.207	1.176	2.62

Comparison between measured and predicted TDG on June 5, 2006

Transect	Easting (feet)	Northing (feet)	Z (feet)	TDG predicted	TDG measured	diff %	Average predicted	Average measured	Average difference (%)
TW1P2	1878138.733	345839.846	648.7	1.160	1.200	-3.38			
TW1P3	1877972.651	345812.512	648.4	1.155	1.180	-2.05			
TW1P4Z1	1877766.08	345652.528	692.0	1.153	1.158	-0.46			
TW1P4Z2	1877685.593	345800.096	657.0	1.152	1.159	-0.68	1.155	1.174	-1.66
TW2P2	1878494.473	343593.521	675.9	1.151	1.181	-2.53			
TW2P3	1878414.713	343618.277	679.9	1.152	1.182	-2.57			
TW2P4	1878237.515	343582.52	698.6	1.151	1.183	-2.73	1.151	1.182	-2.61
WELW	1870372.891	334581.117	692.0	1.149	1.173	-2.04			
TW3P2	1870323.519	334702.235	698.7	1.150	1.178	-2.35			
TW3P4	1870037.256	334948.965	673.4	1.151	1.182	-2.68			
TW3P5	1869929.689	335169.057	697.9	1.150	1.182	-2.67	1.150	1.179	-2.44

Comparison between measured and predicted TDG on May 14, 2006

Transect	Easting (feet)	Northing (feet)	Z (feet)	TDG predicted	TDG measured	diff %	Average predicted	Average measured	Average difference (%)
TW1P1Z1	1878593.614	345704.68	692.0	1.155	1.167	-1.00			
TW1P1Z2	1878511.224	345814.175	669.1	1.159	1.167	-0.67			
TW1P2	1878138.733	345839.846	648.7	1.170	1.181	-0.96			
TW1P3	1877972.651	345812.512	648.4	1.176	1.187	-0.91			
TW1P4Z1	1877766.08	345652.528	692.0	1.173	1.163	0.88			
TW1P4Z2	1877685.593	345800.096	657.0	1.166	1.168	-0.21	1.167	1.172	-0.48
TW2P1	1878645.036	343552.591	675.6	1.162	1.167	-0.43			
TW2P2	1878494.473	343593.521	675.9	1.162	1.170	-0.71			
TW2P3	1878414.713	343618.277	679.9	1.163	1.175	-1.05			
TW2P4	1878237.515	343582.52	698.6	1.164	1.180	-1.38	1.163	1.173	-0.89
WELW	1870372.891	334581.117	692.0	1.163	1.151	1.01			
TW3P2	1870323.519	334702.235	698.7	1.162	1.165	-0.28			
TW3P3	1870104.368	334818.929	679.0	1.163	1.164	-0.12			
TW3P4	1870037.256	334948.965	673.4	1.164	1.173	-0.80			
TW3P5	1869929.689	335169.057	697.9	1.164	1.170	-0.48	1.163	1.165	-0.14

Comparison between measured and predicted TDG on May 17, 2006

Transect	Easting (feet)	Northing (feet)	Z (feet)	TDG predicted	TDG measured	diff %	Average predicted	Average measured	Average difference (%)
TW1-1S	1878593.614	345704.68	692.0	1.147	1.163	-1.38			
TW 1-1	1878511.224	345814.175	669.1	1.156	1.161	-0.44			
TW 1-2	1878138.733	345839.846	648.7	1.183	1.166	1.45			
TW 1-3	1877972.651	345812.512	648.4	1.188	1.173	1.21			
TW1-4S	1877766.08	345652.528	692.0	1.177	1.149	2.47			
TW 1-4	1877685.593	345800.096	657.0	1.168	1.153	1.30	1.170	1.161	0.77
TW 2-2	1878494.473	343593.521	675.9	1.168	1.168	0.01			
TW 2-3	1878414.713	343618.277	679.9	1.171	1.172	-0.11			
TW 2-4	1878237.515	343582.52	698.6	1.167	1.167	0.04	1.169	1.169	-0.02
WELW	1870372.891	334581.117	692.0	1.165	1.153	1.05			
TW 3-2	1870323.519	334702.235	698.7	1.166	1.164	0.15			
TW 3-3	1870104.368	334818.929	679.0	1.167	1.162	0.47			
TW 3-4	1870037.256	334948.965	673.4	1.168	1.169	-0.11			
TW 3-5	1869929.689	335169.057	697.9	1.168	1.161	0.59	1.167	1.162	0.43

Comparison between measured and predicted TDG on June 17, 2006

Transect	Easting (feet)	Northing (feet)	Z (feet)	TDG predicted	TDG measured	diff %	Average predicted	Average measured	Average difference (%)
TW1P1Z1	1878593.614	345704.68	692.0	1.188	1.256	-5.39			
TW1P2	1878138.733	345839.846	648.7	1.398	1.282	12.97			
TW1P3	1877972.651	345812.512	648.4	1.343	1.260	6.57			
TW1P4Z1	1877766.08	345652.528	692.0	1.284	1.217	5.54			
TW1P4Z2	1877685.593	345800.096	657.0	1.259	1.222	3.03	1.305	1.247	4.58
TW2P2	1878494.473	343593.521	675.9	1.261	1.261	-0.02			
TW2P3	1878414.713	343618.277	679.9	1.265	1.261	0.34			
TW2P4	1878237.515	343582.52	698.6	1.265	1.233	2.58	1.264	1.252	0.95
WELW	1870372.891	334581.117	692.0	1.256	1.243	1.06			
TW3P2	1870323.519	334702.235	698.7	1.264	1.249	1.16			
TW3P4	1870037.256	334948.965	673.4	1.268	1.248	1.58			
TW3P5	1869929.689	335169.057	697.9	1.269	1.238	2.53	1.264	1.245	1.58